TWELFTH QUARTERLY REPORT

ON

MOLECULAR CIRCUIT DEVELOPMENT

Period of 15 February 1963 to 15 May 1963

Contract No. NOw 60-0362-C

Submitted to

U.S. Department of the Navy

Bureau of Naval Weapons

Washington 25, D.C.

MELPAR INC.

3000 Arlington Boulevard

Falls Church, Virginia

ULTIMATE PROGRAM OBJECTIVE

The ultimate objective of this program is to acquire the technical knowledge and capability to provide instruction for the formation of complete thin-film circuits and systems in which electronic circuit elements are integrated in a material matrix to a point where individual elemental appearances have been lost. The circuits will be capable of operating at 500°C, and should possess a high degree of radiation resistance. The circuits, as conceived, will contain microareas within a single film and/or be formed of layers of metals, semiconductors, and dielectrics in preconceived configurations to provide the necessary electronic functions. The objective is to be accomplished by performing studies of film and microcrystal formation, surface and interfacial phenomena, and geometric studies of configurations to use, to the maximum advantage, the physical effects that occur in thin films. The electronic circuits so formed will possess a maximum degree of microminiaturization.

TABLE OF CONTENTS

		Page
1	INTRODUCTION	5
2.	MATERIALS RESEARCH	7
	2.1 Chemical Vapor Deposition of Semiconductive Films	8
	2.2 Deposition of II-VI Compounds	13
	2.3. Sputtered Semiconductive Films	17
	2.3.1 Sputtered Silicon Carbide Films	17
	2.3.2 Other Sputtered Materials	20
	2.3.3 Conclusions	21
	2.4 Dielectric Films	23
	2.4.1 Introduction	23
	2.4.2 Deposition of Neodymium Oxide	23
	2.4.3 Film Structure and Composition	24
	2.4.4 General Properties of Nd_2O_3 Films Deposited from Boron Nitride Liners	25
	2.4.5 Thickness Dependence of the Electrical Properties of Nd_2O_3	25
	2.4.6 Frequency Characteristics of Nd_2O_3 Capacitors	27
	2.4.7 Temperature Dependence of the Electrical Properties of Capacitors	34
	2.5 Boron Films	39
	2.5.1 Deposition Techniques	39
	2.5.2 Electrical Properties	41
	2.5.3 Discussion	43

TABLE OF CONTENTS (Continued)

		Page
3.	MICRODEVICE RESEARCH	48
	3.1 Thin-Film Device Characteristics	48
	3.2 Thermal Properties of Thin-film Devices	51
4.	FUNCTION SYNTHESIS STUDIES	52
	4.1 A Current Limiter Application of the Thin-Film Triode	52
5.	CONCLUSIONS	62

LIST OF ILLUSTRATIONS

Figure		Page
1.	Photomicrographs of SiC Deposits on Aluminum Magnesium Silicate Substrates	9
2.	Vapor Pressure Curves of Elements in Some II-VI Compounds (after R. Honig)	14
3.	Field Effect Sensitivity vs. Semiconductor Deposition Rate	16
4.	I-V Characteristic of Sputtered SiC Film	19
5.	Thickness Dependence of Dielectric Constant of Nd_2O_3 Deposited from Metal Boats	26
6.	Dissipation Factor and Dielectric Constant versus Thickness	28
7.	Frequency Dependence of an Nd_2O_3 Capacitor at Room Temperature	29
8.	Frequency Characteristics of an Nd_2O_3 Capacitor at Various Temperatures	30
9.	Dissipation Factor and Dielectric Constant vs. Temperature	35
10.	Dielectric Breakdown Strength vs. Temperature	38
11.	I-V Characteristics of a Boron Three-Layer Device	42
12.	I-V Characteristics of a Boron Three-Layer Device at Several Temperatures	44
13.	Schematic Diagram and Input and Output Wave Forms of Clipping Circuit using a Boron Three-Layer Device	45
14.	I-E Characteristics of Several Amorphous Materials	46
15.	I_D-V_D Characteristics of a CdSe Device Operating in the Enhancement Mode	49
16.	Depletion Layer in Self-Biased Field Effect Unit	53
17.	I-V Characteristic of the Current Limiter	55

1. INTRODUCTION

This Twelfth Quarterly Report on Molecular Circuit Development is submitted in compliance with Contract NOw-60-0362-c. The purpose of the program, as set forth in the Ultimate Program Objective, is to conduct research and development on materials and techniques suitable for the formation of molecular circuits. The program is divided into major research efforts associated with materials and microdevices.

Material research is currently engaged in the study of semiconductive films of silicon carbide, boron, and cadmium selenide and of dielectric films of neodymium oxide. Chemical vapor depositions have been successful in producing various types of crystallites and crystalline aggregates of silicon carbide; experiments aimed at obtaining uniform films have been continued.

Amorphous boron films, deposited by means of electron beam evaporation, have proved useful in the study of electron transmission through thin films. Results of this research indicate that amorphous films might possess valuable properties quite distinct from those representative of the crystalline state. An operating clipping circuit based on conduction through a boron film has been devised.

Investigations of dielectric films have been concerned with the characterization of neodymium oxide. Deposition procedures have been carefully investigated, and electrical properties evaluated over a wide temperature range. This material shows excellent capabilities for use as a high temperature dielectric.

Under microdevice research, work on field effect devices continues apace. Cadmium selenide remains the preferred material for the semiconductor film. An

effect due to the type of dielectric material used has been observed, and investigations in this area are underway. The application of a field effect device in a current limiter circuit has been studied for the purpose of comparing experimental results with certain theoretical predictions.

Samples of completely deposited oscillators and flip-flops using field effect devices were sent to Hughes Aircraft Co. for radiation tests and the extremely promising results will be contained in the Hughes reports.

2. MATERIALS RESEARCH

As in the past, the principal efforts in the field of materials research are directed toward study of semiconductive and dielectric films. The recent emphasis in semiconductors has been on those materials which would be especially suitable for high temperatures. Depositions of silicon carbide have been approached by means of both the chemical vapor and cathodic sputtering techniques. Various types of silicon carbide crystallites have been formed by vapor plating at high temperatures. The sputtered films have invariably been amorphous, and attempts to crystallize them in thermal treatments have been fruitless. The chemically formed crystalline deposits are more promising in this respect.

Experimentation on evaporated boron films was renewed this quarter. Rather than attempt to crystalize the films, they have been studied in an amorphous state. Investigations of their electronic conduction have intimated that potentially profitable results are achievable from such an approach. A simple clipping circuit using such a film was constructed and its operation demonstrated.

Despite exploratory work with deposition of a variety of II-VI semiconductive compounds, none allowed production of field effect devices having such favorable properties as cadmium selenide. Greater reliability has been abhieved as a result of a study of deposition rate.

The films formed from neodymium oxide have proved to be practicable as the dielectric for thin film capacitors operable to 500°C. The conditions of vacuum deposition are especially important for obtaining satisfactory dielectric properties; this is undoubtedly related to the exact chemical constitution of the films, although it has not yet been completely indentified.

2.1 Chemical Vapor Deposition of Semiconductive Films

During this quarter, investigations of the chemical vapor deposition of silicon carbide through the pyrolysis and/or reduction of tetraethylsilane were initiated. Photomicrographs of these deposits are in many respects exact replicas of those which appear in the classical literature (see figure 1). However, the yields have been low. The recent effort has been directed towards the production of thin films, rather than whiskers, platelets, or crystalline aggregates which have formed. Except for slight modifications in the reaction chamber, the apparatus used in these experiments has been described previously (See Ninth Quarterly Report, pages 11-15, and figure 3). In the initial exploratory work, thirty-four experiments have been performed. These experiments have revealed the following:

a. Silicon carbide crystallites can be formed along the highly active edges of alumina at temperatures below 1000°C. These were revealed as mushroom-shaped clusters of mixed green and blue-black crystals.

b. Films formed on the substrates thus far evaluated are primarily of low resistance, but show no observable Hall or field effects.

c. The chemical and physical nature of the substrate appears to be an important parameter affecting the extent and type of growth, since two-dimensional colored films and mushroom-shaped clusters have been observed. Substrates thus far used include fused quartz, AlSiMag-614, high purity alumina, and Pyroceram (Code 9606).

d. The angle of incidence (gas stream versus substrate) has an important bearing on the nature of the deposit, as well as on the kinetics of the crystal growth. Clusters whose heights exceed 1/8 inch are now being analyzed.

(a) SiC FILM (RUN 33)-400X

(b) SiC CRYSTALLITES (RUN 31)-400X

(c) SiC NEEDLES (RUN 28)-100X

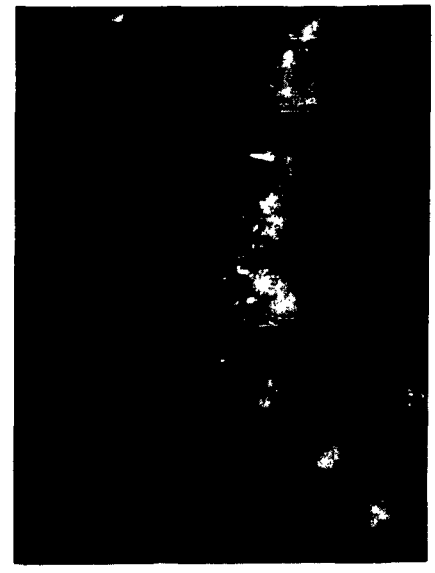

(d) SiC NEEDLES ON SUBSTRATE EDGE (RUN 28)-100X

Figure 1. Photomicrographs of SiC Deposits on Aluminum Magnesium Silicate Substrates

e. The optimum deposition temperature depends upon other parameters, such as the concentration of the gas stream, its angle of incidence, the substrate material, and perhaps the stream velocity.

f. The presence of hydrogen in the feed gas (helium plus tetraethylsilane) with all other conditions remaining constant, has thus far produced no variations in the deposited films.

The data for the thirty-four experiments appear in table 1.

The next phase of this investigation will be directed towards optimizing the conditions for film growth by a more penetrating and critical study of variables such as the substrate, angle of incidence, stream velocity, concentration, and temperature. Although the above work was performed within the interval of 850-1650°C, the capability exists to go even higher.

Also during the next quarter, work will commence on the behavior of chlorine-containing alkyl silicon compounds. No attempts have been made to elucidate reaction mechanisms to date.

TABLE I

Chemically Deposited Silicon Carbide Films

Run No.	Subst Temp °C	Depos. Time (min)	Conditioning Gas	Carrier Gas	Carrier Gas Flow Rate 1/m	Linear Vel. cm/sec	Vapor Conc. % mole	Substrate Material	Remarks
1	950	30	He	He	0.80	17	1.14	Fused Quartz	Gray metallic film. Conductive. Discontinuous in some areas.
2	965	30	He	He	0.80	17	1.14	Fused Quartz	Gray metallic film. Conductive but discontinous. Poor adhesion.
3	965	30	He	He	0.80	17	1.14	Fused Quartz	Metallic blue-black film. Conductive but discontinuous.
4	995	30	He	He	0.80	17	1.14	Fused Quartz	Gray metallic film. Conductive. Adhesion in central area, peeling on edges.
5	990	20	He	He	0.80	17	1.14	Fused Quartz	Shorter deposition time did not reduce cracking and peeling. Film unaffected by HF or HF + HNO_3 solution.
6	1000	30	He	He	0.80	17	1.14	Fused Quartz	Gray metallic film. Highly conductive.
7	1000	15	He	He	0.80	17	1.14	Pyroceram	Adherent smooth gray-black film. HF and HF + HNO_3 test negative. Film has the appearance of pyrolytic graphite.
8	1000	30	He	He	0.80	17	0.57	Pyroceram	Adherent smooth gray-black film. Acid test negative Flame test positive. Oxidation noticeable. Carbon.
9	1212	20	He	He	0.80	17	1.14	Pyroceram	Thin deposit in central area. Carbonaceous deposits on edges. % film composition determination anomalous.
10	1000	30	He	He	0.80	17	0.57	Pyroceram	Gray metallic film. Run made to determine total am't of deposition versus time and vap. conc. See run no. 7 for conditions. Weights: No. 7 0.0045 g +, No. 10 0.0044 g +
11	1000	30	He	He	0.80	17	1.14	Pyroceram	Small am't of deposition. Gray met'lic film. Wet analysis inconclusive.
12	1220	30	He	He	0.80	17	1.14	Pyroceram	Max op temp of pyro'm. Subst. melting.
13	895	30	He	He	0.80	17	1.14	Pyroceram	Small am't of deposition. Thin adherent film of various hues.
14	1290	30	He	He	0.80	17	1.14	Pyroceram	Subst decomp. Material discontinued.
15	900	30	He	He	0.80	17	1.14	Fused Quartz	Very thin translucent yellow film.
16	1400	40	He	He	0.80	17	1.14	Al_2O_3 tubing	Subst. was 1/2 ceramic tube with sharp edges exposed to vapor flow. Gray metallic deposit. Tube edges had mushroom and spicular formations.
17	1550	40	He	He	0.80	17	1.14	Mo	Gray film with numerous hillocks.

TABLE I (continued)

Run No.	Subst Temp °C	Depos. Time (min)	Conditioning Gas	Carrier Gas	Carrier Gas Flow Rate 1/m	Linear Vel. cm/sec	Vapor Conc. % mole	Substrate Material	Remarks
18	1500	60	He	He	0.80	17	1.14	Al_2O_3 chips	Gray film with a metallic sheen. Mushroom and spicular formations. Appears to be graphite. Black C on edges.
19	1450	60	He	He	0.80	17	1.14	Fused Quartz	Thin gray metallic film. Peeling and cracking on edges.
20	1550	30	He	He	0.80	17	1.14	AlSiMag 614	Dark gray film. No adhesion.
21	1570	50	He	He	0.80	17	1.14	AlSiMag 614	Gray silvery metallic film. No adhesion.
22	1500	15	He	H_2	0.80	17	1.14	AlSiMag 614	Very thin discontinuous film of a purplish blue-black color. Adherent but some discontinuities in evidence on edges.
23	1400	30	He	H_2	0.80	17	1.14	AlSiMag 614	Thin film flaking off on edges.
24	1610	60	He	He	0.70	14.8	0.57	AlSiMag 614	Thin smooth adherent gray film with a metallic sheen. No peeling or cracking.
25	880	30	He	H_2	0.80	17	1.14	Fused Quartz	Reducing atmosphere and low temperature Nonconductive thin translucent yellow film. Appears to be organic residues.
26	1035	30	He	H_2	0.80	17	1.14	Fused Quartz	Conductive thin dark bluish film, shiny in one corner and dull in other areas. Hillocks and cracking. Discontinuous.
27	1315	30	He	H_2	0.80	17	1.14	Fused Quartz	Thin peeling conductive film. Extensive peeling and hillocks. Subst melting.
28	1650	30	He	He	0.80	17	1.14	Al_2O_3 614	Gray black adherent film. Pictures show typical SiC formations. Weight loss.
29	1525	30	He	He	0.80	17	1.14	Al_2O_3 614	Reactor cleaned and system preconditioned Poor film due to residual moisture on reactor walls. Extensive peeling and cracking. Weight loss.
30	1550	30	He	He	0.80	17	1.14	Al_2O_3 614	Conductive gray film with a metallic sheen. Adherent initially but peeled off completely after 24 hours. Pentecost.
31	1575	60	He	He	0.80	17	1.14	Al_2O_3 614	Polycrystalline formations underneath substrate. Substrate warped. Pictures showing definite crystalline formation with dislocations inherent in SiC. α SiC confirmed.
32	1105	30	He	He	0.80	17	1.14	Fused Quartz chips	Gray silvery porous deposit. Unaffected by HF or HF + HNO_3 but partially dissolved by H_2SO_4 + HNO_3 (4 hrs).
33	1530	30	He	He	0.80	17	1.14	AlSiMag 614	Angle of incidence 60°. Gray metallic tap half adherent even deposition. Yellow formations on lower portion.
34	1530	30	He	He	0.50	10.6	1.14	AlSiMag 614	Adherent smooth even film, metallic gray in color weight loss. Conductive.

2.2 Deposition of II-VI Compounds

Efforts were also concentrated on CdSe films, since devices utilizing this material have consistently shown characteristics superior to those of CdTe and CdS units.* With regard to the formation techniques discussed in the previous report, it appeared that CdSe devices were more easily formed, with considerably better reproducibility. One possible clue as to why this should be so can be found in the relative vapor pressure curves of Honig[1] (See figure 2). It is not known exactly to what extent dissociation of a compound accurs in the vapor phase, but this probably depends largely on the rate of evaporation, which is related to source temperature. Several investigators of CdSe[2,3] have indicated that complete dissociation of the material occurs in the vapor phase, while others have suggested that dissociation of CdS is dependent on the source temperature.[4] Our work has also indicated dissociation of these materials, as shown by an excess of one or the other of the constituent elements found in various films (See 11th Quarterly Report).

If dissociation does occur, it is reasonable to assume that the nearly identical vapor pressures of Se and Cd, as read from Honig's curves, lead to a more congruent evaporation of these two elements than would be the case for the constituent elements of either CdS or CdTe. Experiments of

---

* For convenience, devices are identified in these reports with the semiconductor layer used, i.e. devices utilizing a CdS layer will be identified as CdS devices; units with CdSe layers as CdSe devices, etc.

1. R.. Honig, RCA Review 23, 567 (1962).
2. D. DeNobel, Ph.D. Thesis, University of Leiden (1958).
3. P. Goldinger et al., Tech Rept., Univ. Libre Bruxelles, Jan. 1959.
4. E. Senkovits and R. Zuleeg, Electrochemical Soc. Mtg., Pittsburgh, Pa., April, 1963.

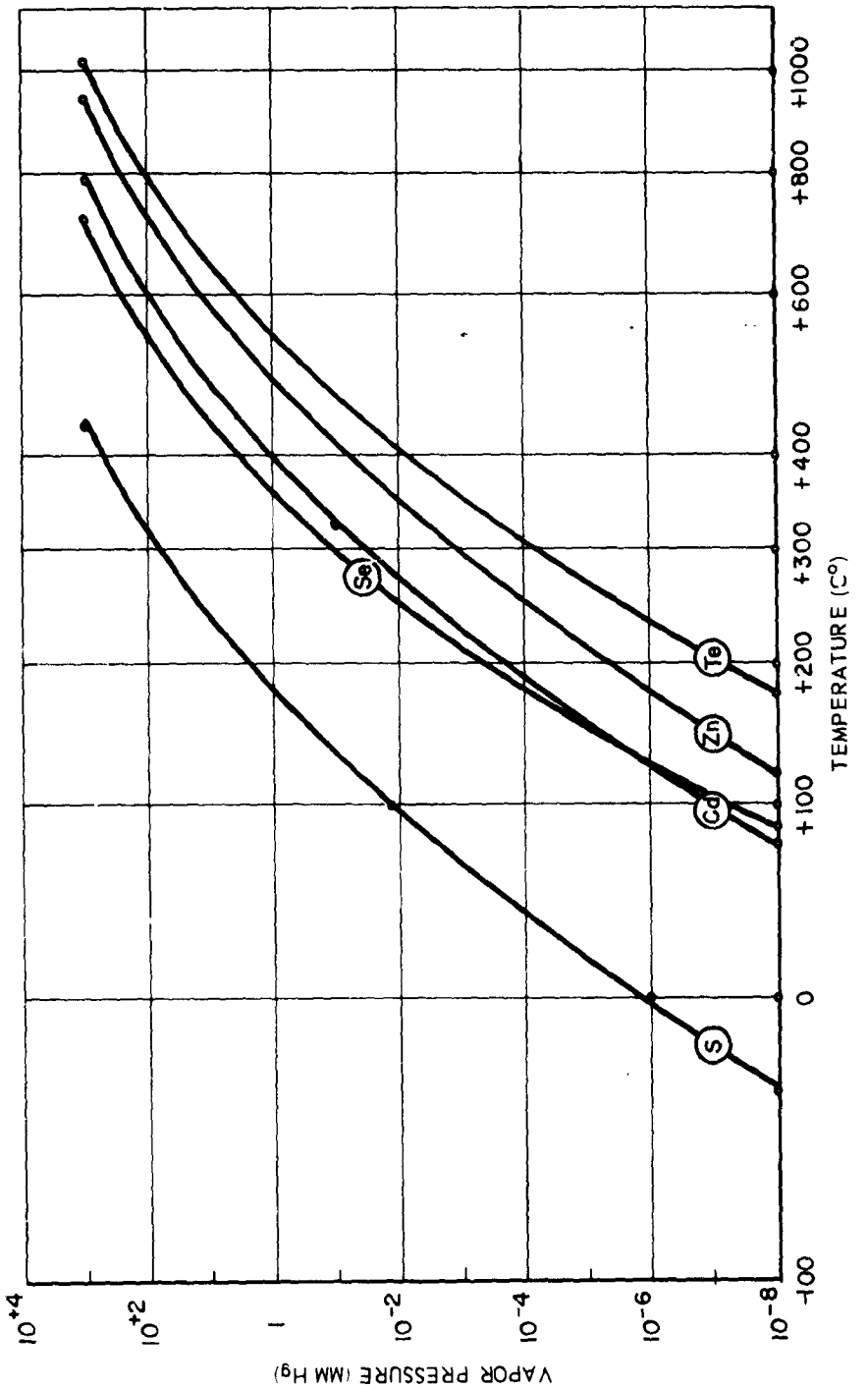

Figure 2. Vapor Pressure Curves of Elements in Some II-VI Compounds (after R. Honig)

Somorjai[5] on the determination of equilibrium vapor pressure and dew point data for CdSe have indicated that this material vaporizes congruently. Assuming further that the sticking coefficients are the same at the deposition conditions, it is possible to foresee a more nearly stoichiometric ratio for films of the selenide than for either the sulfide or telluride.

Among the many deposition parameters which have been found to influence the sensitivity of CdSe devices is the rate of deposition. Figure 3 is a plot of relative field effect (in arbitrary units) versus the rate of evaporation at which the CdSe layer was deposited. Higher sensitivity to field effect was found in devices for which the CdSe layer was deposited at rapid rates (i.e. $>$ 5000 Å /minute). For these faster depositions splitting of the CdSe source material occurs, resulting in loss of material and/or collection of large particles on the substrate. The reason for this lies in the volatile nature of the CdSe material and the relatively high boat temperatures required for the faster deposition rates. In order to prevent splitting, a cone extension of the boat, insulated electrically and thermally, is utilized. This cone is topped by a filter of fused quartz fiber. This arrangement is used with a tungsten boat and sintered CdSe polycrystalline cake as the source material. In the evaporation of CdSe powder, a somewhat different arrangement is made, the CdSe powder being packed slightly into a graphite boat and a fused quartz wool plug or fiber filter placed over the top. Use of various oxide liners to prevent reaction of the CdSe with the boat material has not resulted in any notable improvement to the devices.

---

5. G. A. Somorjai, J. Phys. Chem. 65, 1059 (1961).

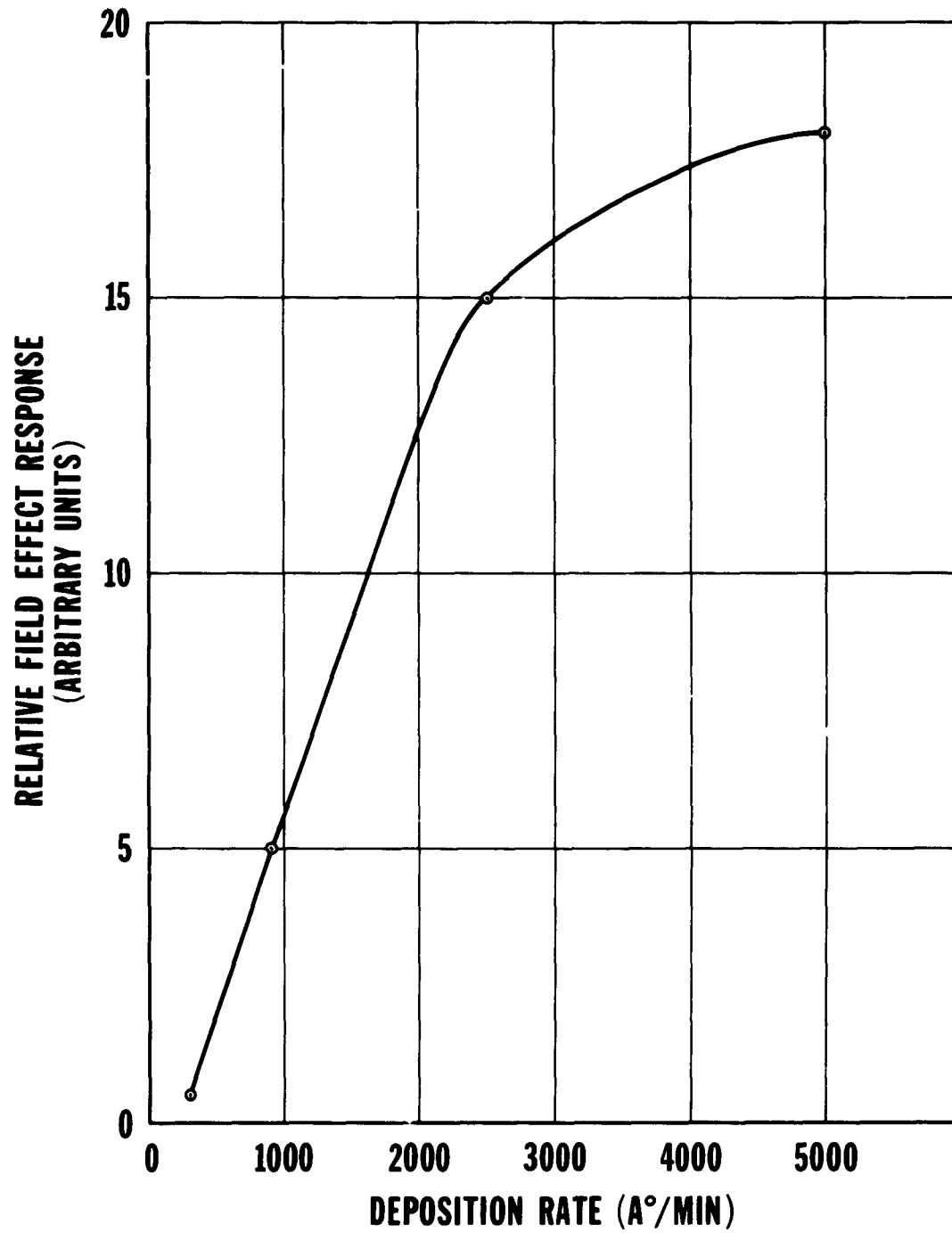

Figure 3. Field Effect Sensitivity vs. Semiconductor Deposition Rate

2.3 Sputtered Semiconductive Films

2.3.1 Sputtered Silicon Carbide Films

Silicon carbide films were sputtered into several configurations suitable for various types of evaluation; these have included narrow channel, capacitor, electron transmission, field effect, as well as the more usual Hall sample configuration. The narrow channel and capacitor-like arrangements were used in attempts to get realistic resistance measurements of the SiC films through small dimensions. The channel was formed by leaving a gap of some 10-15 mils between metallic contact tabs of aluminum or Nichrome, the SiC film being deposited in the form of a transverse strip, filling the channel and overlapping the electrodes. For the capacitor-like arrangement, the sputtered films were deposited in the usual way over a large bottom electrode and the top plates finally applied. The transmission samples were constructed with the sputtered film situated between crossed arrays of metallic strips, the top set perpendicularly to the bottom, forming a grid arrangement. Resistance readings are then made through the films, which may be up to several thousand angstroms in thickness, at any of the points of intersection of the grid described in Section 2.5.

Most of the SiC films were sputtered from the Exolon Co. source material previously described, but a few prepared at the end of the quarter were formed from chips of 99.95% purity, obtained from Kern Chemical Co.

Several SiC films were given heat treatments under argon of 1120°C and 1250°C for various periods of time. These films were then examined by means of X-ray diffraction.

DC voltage-current characteristics were determined for the electron

transmission samples. The applied EMF ranged approximately from 0.1 to 50 v.

Several films were sputtered from an ultra high purity boron source, reported to have a purity of 99.9999%, supplied by the Eagle-Picher Co. One of these films was included in the group of samples heated at 1250°C for 8 hours.

Two films were also formed by sputtering from a sample of aluminum antimonide, procured from Penn Rare Metals, Inc.

For the most part, the sputtered SiC films have been extremely high in resistance, as measured along the major film dimensions. In the few cases for which fairly low resistance values had been observed, it is now presumed that considerable impurities had entered the film, probably from the rather impure source materials. It is noteworthy that these samples of relatively low resistance were also invariably discolored, dark brown to black, as compared with the pale yellow of the high resistance films; the discolorations were also generally non-uniform, displaying rather irregular patterns throughout the films.

Determination made on the electron transmission samples demonstrated that these highly resistive films possess measurable values of the resistance. One such measurement, a voltage-current characteristic for the sample S-SiC-30, with a film of 4000 Å thickness, is depicted in figure 4; the same data are plotted in figure 14, displayed as a field-current characteristic. This characteristic, evaluated at one of the grid intersections, gives no indication of a break, as has been observed with evaporated boron films, but represents rather a smooth, slightly non-ohmic dependence of current on voltage. The calculated resistance is some 20 megohms. Such behavior has been typical of all of the transmission samples.

Since measurable values of resistance could be read through the narrow dimensions of the films, it was decided to deposit into narrow channels separating metal contact tabs. However, the films obtained were still generally extremely

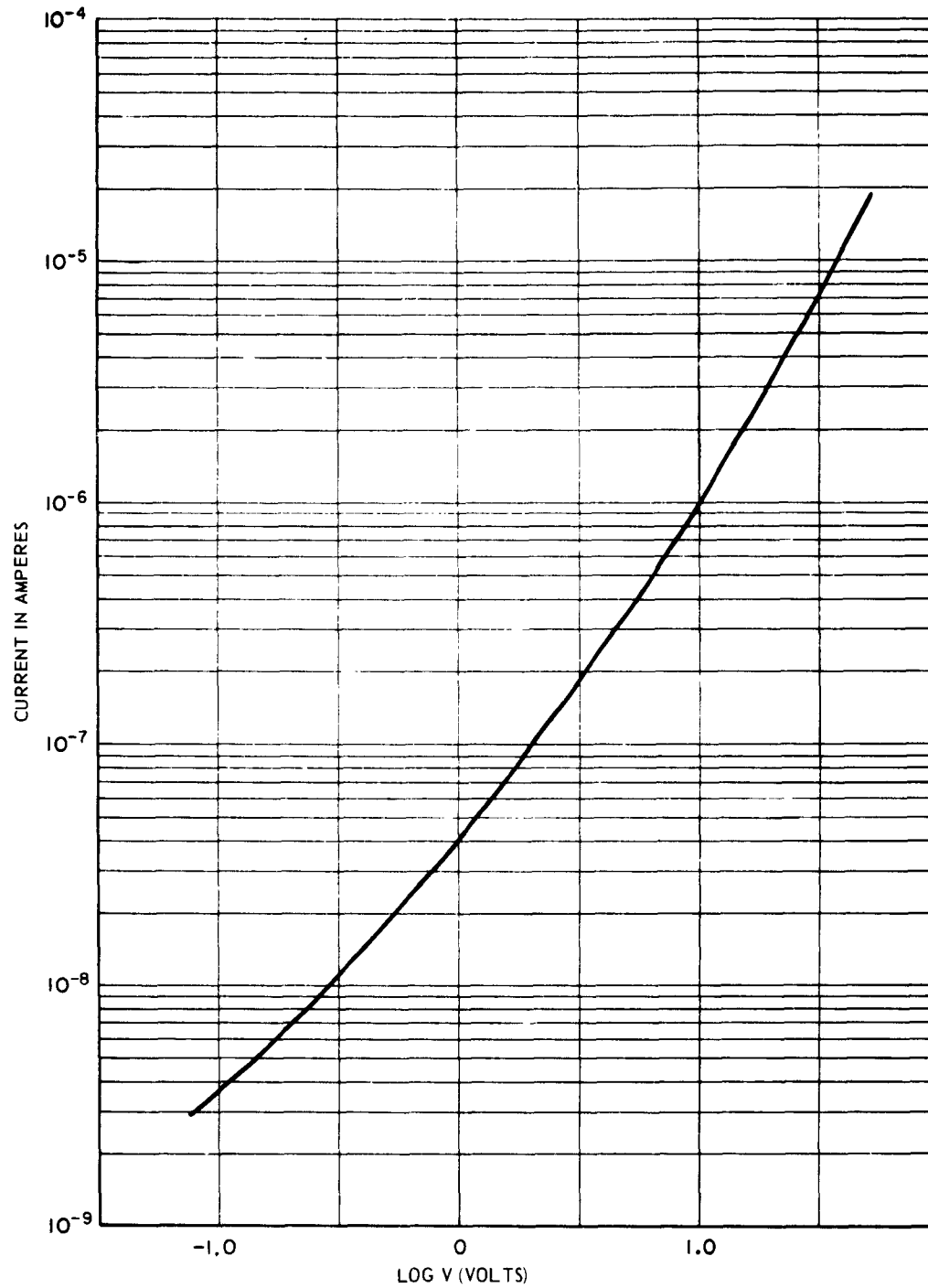

Figure 4. I-V Characteristic of Sputtered SiC Film

high in resistance ($>10^{11}$ - $10^{12}\Omega$). The capacitor-like configuration did not prove to be suitable, because of frequent shorting through pinholes in the sputtered film.

In no case has it been possible to make any Hall effect measurements this quarter, because of the extremely high resistance values.

Use of the source material obtained from Kern Chemical Co. proved to be of no advantage in forming sputtered films.

. . Of the three samples subjected to the prolonged treatment at 1120°C (23 hours), S-SiC-6 and 10 had previously been heated, at 1170° and 1000°C respectively. As a result of 1120° treatment, there appeared to be some crazing; the X-ray diffraction patterns suggested the presence of a high temperature form of silica, but gave no indication of a crystalline form of silicon carbide. The third sample of this group, S-SiC-28, volatilized completely during the treatment; this film was considerably thinner than the other two as originally deposited - some 2000 vs. 4000 and 5000 Å, a factor which undoubtedly explains its more ready loss due to volatilization. Both of the films given the 1250° for 8 hours treatment, S-SiC-32 and 35, also virtually completely volatilized; at 1120° for 8 hours these films had given no indications of any changes.

2.3.2 Other Sputtered Materials

Preliminary experiment on sputtered boron and AlSb were initiated. Of the several films deposited from the boron source, little is yet known. X-ray diffraction has not confirmed boron, presumably because of an amorphous structure, but in one case a single peak which corresponds to the principal line of B_2O_3 was found. It may be that these films are quite sensitive to air oxidation. All films were extremely high in resistance ($>10^{12}\Omega$), generally transparent and clear

in appearance. Thicknesses ranged up to about 4000Å. The one film that was heat-treated crazed extensively, probably because of thermal expansion mismatch with the fused silica substrate, and may have volatilized to some extent; no lowering of resistance or crystallization was apparent.

Three films were sputtered from the AlSb source. Two of these were discolored and non-uniform in appearance. The third, however, was metallic in appearance, with a probe resistance of 20 MΩ and n-type conduction; resemblance to intermetallic compounds previously reported indicates that the film was aluminum antimonide. However, none of these films gave an X-ray diffraction pattern.

2.3.3 Conclusions

Because of the lack of success in forming sputtered silicon carbide films of value, work with this material is being halted. A report by Honig[6] indicates that the sputtering process for silicon carbide is extremely complicated, many molecular species - neutral, positively and negatively charged- being produced in the bombardment. It then appears that films of good reproducibility would be virtually impossible to form by means of sputtering.

Further, the volatilization of the films well below 1200°C makes it extremely unlikely that the amorphous films could be adequately crystallized in any practicable heat treatment. Volatility at these temperatures was not expected, but only small amounts of oxygen in the argon atmosphere would be required

---

6 R. B. Honig, in H. Maecker, Ionization Phenomena in Gases, Vol. I, 106, North-Holland Publ. Co., Amsterdam (1962).

to account for the loss; [7] in this connection, the indicated presence of SiO_2 in some of the heat treated films is probably significant. It has also been suggested that the gaseous molecule SiC_2 might be of importance in the vaporization of silicon carbide. [8]

---

7 G. Ervin, Jr., J. Am. Ceram. Soc. 41, 347 (1958)

8 J. L. Margrave, in J. O'M Bockris, J. L. White, and J. D. Mackenzie, Physicochemical Measurements at High Temperatures, 356, Butterworths Scientific Publications, London (1959).

2.4 Dielectric Films

2.4.1 Introduction

A dielectric material for use in capacitors operable at 500°C has been found this quarter. The film properties are strongly dependent on the film composition, which is in turn found to be dependent on the deposition technique. Only those films deposited from a boron nitride crucible liner show the desired temperature characteristics.

2.4.2 Deposition of Neodymium Oxide

Capacitors have been formed and studied this quarter using neodymium oxide as the dielectric material. The source material was in the form of pellets, pressed from 99.999 percent pure Nd_2O_3 powder [9] at 15,000 lbs/sq.in. After pressing, the pellets were heated to 300°C to remove moisture. The material was evaporated from metal boats of tantalum and tungsten, from boron nitride liners in graphite heaters [10] and by electron beam heating. An unusually rapid increase in vacuum chamber pressure during the preliminary heating-up process indicated that the Nd_2O_3 was dissociating and/or outgassing well below the evaporation temperature of the material (2350°C). Of the various techniques employed, the graphite heater with the boron nitride liner provided the best dielectric films, exhibiting such characteristics as low loss, low dielectric constant, high dc breakdown strength, and high resistivity.

Films of Nd_2O_3 deposited from metal boats had a tendency to be reduced. The films were dark in color exhibited low resistivity, high pinhole density, and high dielectric constant and dissipation factor. These characteristics

---

9 American Potash and Chemical Company

10 F. J. Hemmer and J. R. Piedmont, Rev. Sci. Inst., Vol. 33, 12, (1962).

could be altered appreciably if the film was heated in air. After heating, the film was clear, there were much fewer shorts due to pinholes and the dielectric constant and dissipation factor could be reduced by 10 to 30%. This indicated a strong dependence of these electrical properties on the degree of oxidation.

Films of Nd_2O_3 evaporated by electron beam heating were also reduced, due probably to the proximity of the carbon support. They were all characterized with a large pinhole density and high loss. Zirconium oxide liners are currently being tested but data are incomplete and will be reported next quarter.

2.4.3 Film Structure and Composition

The film samples evaporated from the boron nitride liner formed very clear films at relatively rapid rates of evaporation. A very high yield of pinhole-free capacitors as low as 200 Å in thickness indicates that the material readily forms continuous and homogeneous layers. X-ray diffraction and electron diffraction studies were made of films deposited on fused silica substrates and carbonized copper screens, respectively. Samples for both techniques were deposited on surfaces held at temperatures up to 400°C. The results of the diffraction studies indicated that the films were amorphous, and crystal growth could not be initiated during deposition at these temperatures. Further diffraction studies indicated that crystal growth was not enhanced by subsequent annealing cycles to 500°C. Neodymium was positively identified as a major element by both emission spectrography and X-ray fluorescence techniques. The major impurity present in the films is boron, with traces of calcium, magnesium, and copper. During the next

quarter, identification techniques will be extended to microanalysis and optical absorbtion.

2.4.4 General Properties of Nd_2O_3 Films Deposited from Boron Nitride Liners

An evaporation temperature of 2350°C, measured with an optical pyrometer was found to give condensation rates up to 16 Å per second for films deposited from a boron nitride liner 5 inches from the substrate. The films deposited under these conditions were clear and formed pinhole-free layers in thicknesses as low as 200 angstroms. The thicker films are highly stressed and cracked easily at high temperatures, whereas the thinner films are affected by moisture in the atmosphere and are soluble when immersed in water. It is therefore necessary to protect the capacitors by potting immediately after deposition. The electrical properties were not found to be dependent on the substrate temperature during deposition although film cracking was observed to be less pronounced for films deposited at substrate temperatures above 400°C. For convenience, the capacitors were formed at about 150°C.

The dielectric constant for films deposited from BN liners, was found to be insensitive both to the thickness of the film and to metal electrode material. It is also independent of frequency from 100 cycles per second to 10 megacycles per second and of temperature from -200°C to 500°C.

2.4.5. Thickness Dependence of the Electrical Properties of Nd_2O_3 Films

Figure 5 shows the thickness dependence of the dielectric constant of the films evaporated from metal boats. The dielectric constants of the films deposited from the tantalum boats are smaller than those of films deposited from tungsten boats. Since we have experimentally verified the lowering of dialectric constants by oxidation, we infer that there is more oxide in the films deposited from the tantalum boats.

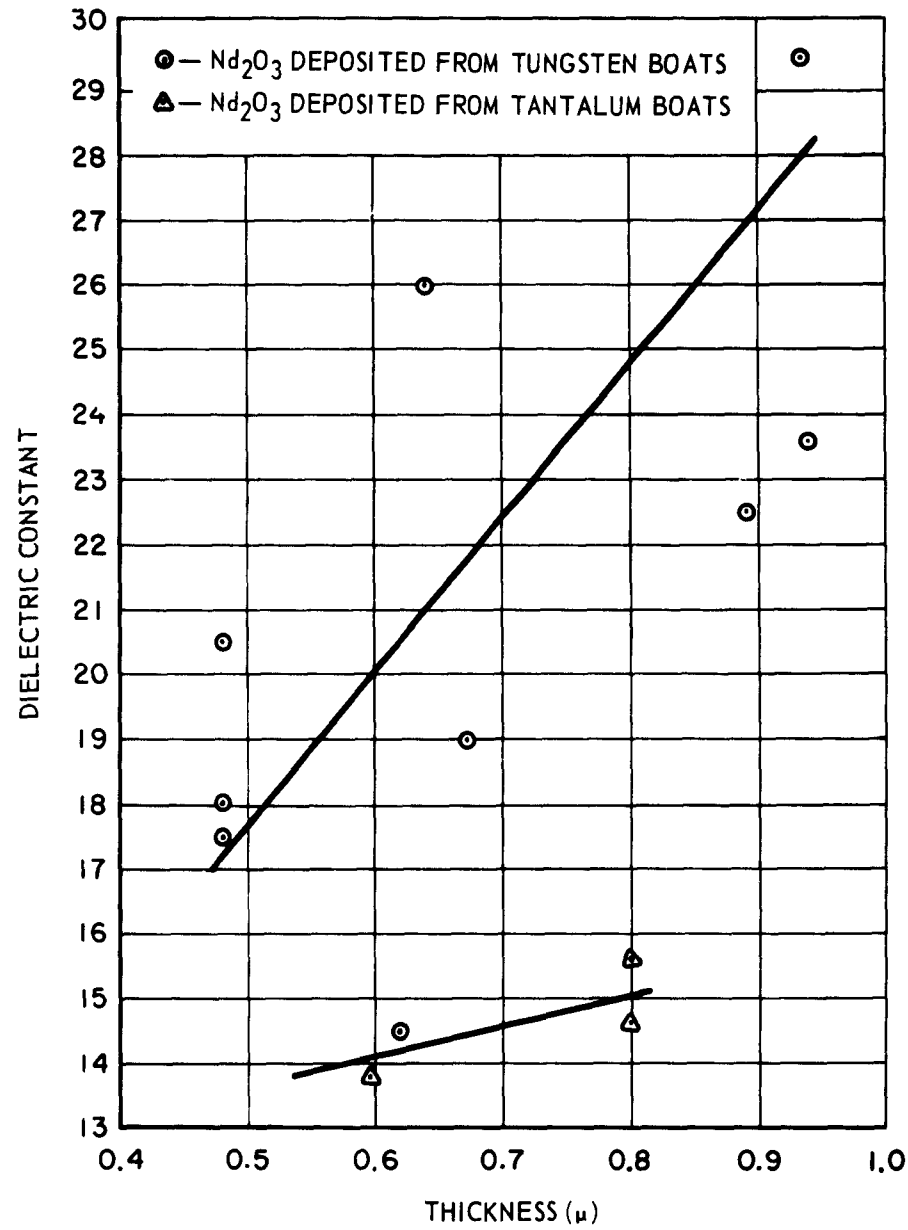

Figure 5. Thickness Dependence of Dielectric Constant of Nd_2O_3 Deposited from Metal Boats

In figure 6, the thickness dependence of both the dissipation factor and the dielectric constant of films deposited from boron nitride liners in graphite crucibles is shown. The large scatter of the data is believed to be a function of the degree of oxidation. The films formed at slower condensation rates were found to have higher dielectric constants. This rather indirectly verifies the idea of oxidation dependence, in that the slower the condensation rate with respect to the rate of dissociation, the less the oxide formation at the substrate and the less the oxygen content of the evaporant. This is due to the fact that released oxygen is pumped out of the vacuum system or is combined with the boat material faster than it can recombine with elemental neodymium at the substrate. Thus, with less oxygen in the film, there results a higher dielectric constant. Dielectric constants below 3.0 are assumed to correspond to fully oxidized films.

2.4.6 Frequency Characteristics of Nd_2O_3 Capacitors

Studying the frequency characteristics of thin-film capacitors offers a convenient way to separate the loss of the dielectric and that of the leads and electrodes while also giving a criterion for comparison of properties of capacitors using different dielectric or electrode materials.

Some typical frequency characteristics of the loss at various temperatures are displayed in figures 7 and 8 for capacitors with Nd_2O_3 layers evaporated from BN liners. In order to understand the significance of this behavior, consider the series equivalent circuit for a thin-film capacitor shown in figure 7. The measured dissipation factor, or $\tan\delta$ of this capacitance-resistance series network is given by

$$\tan\delta \approx \omega C(R_S + R_D) \qquad (1)$$

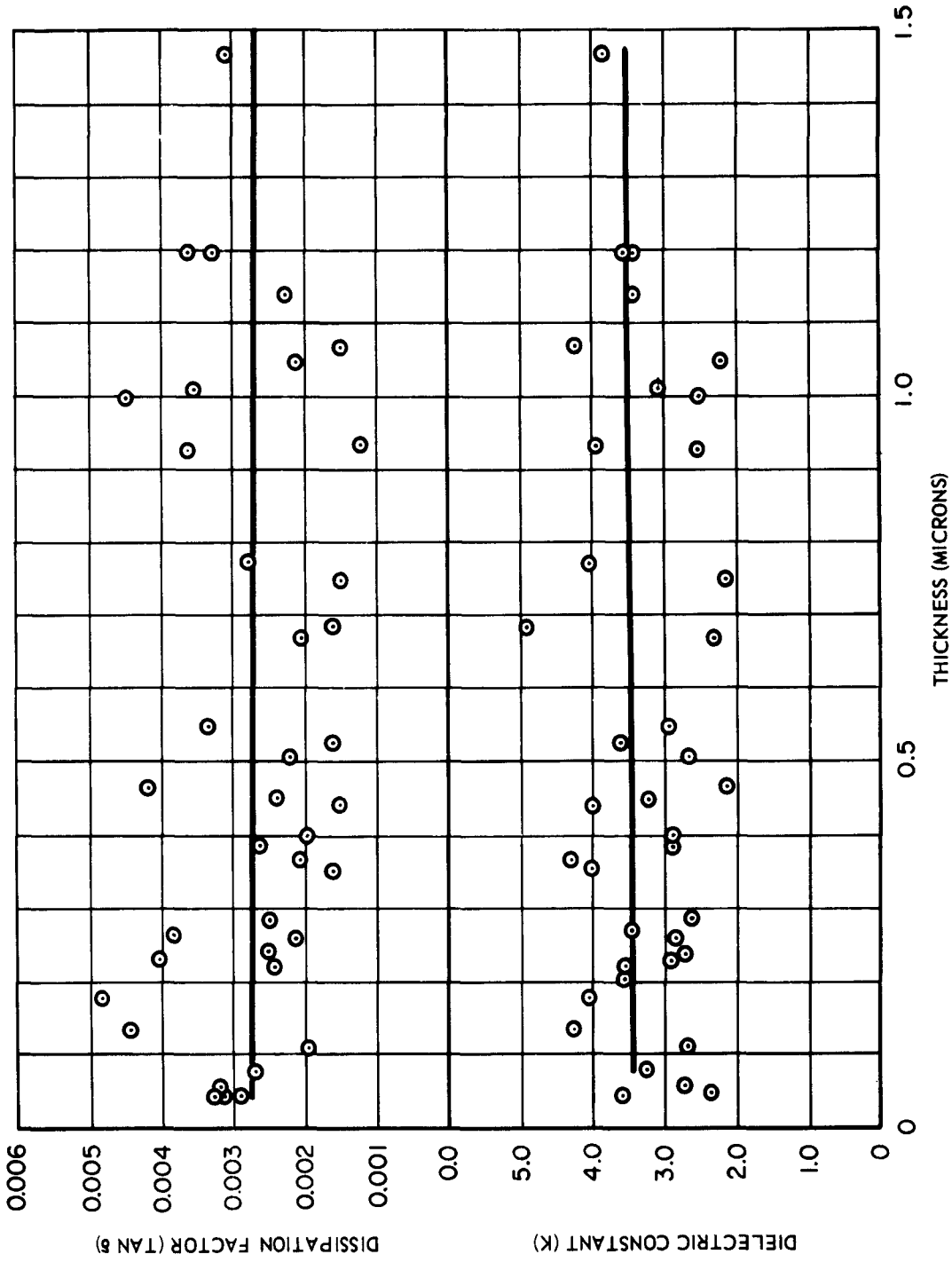

Figure 6. Dissipation Factor and Dielectric Constant versus Thickness

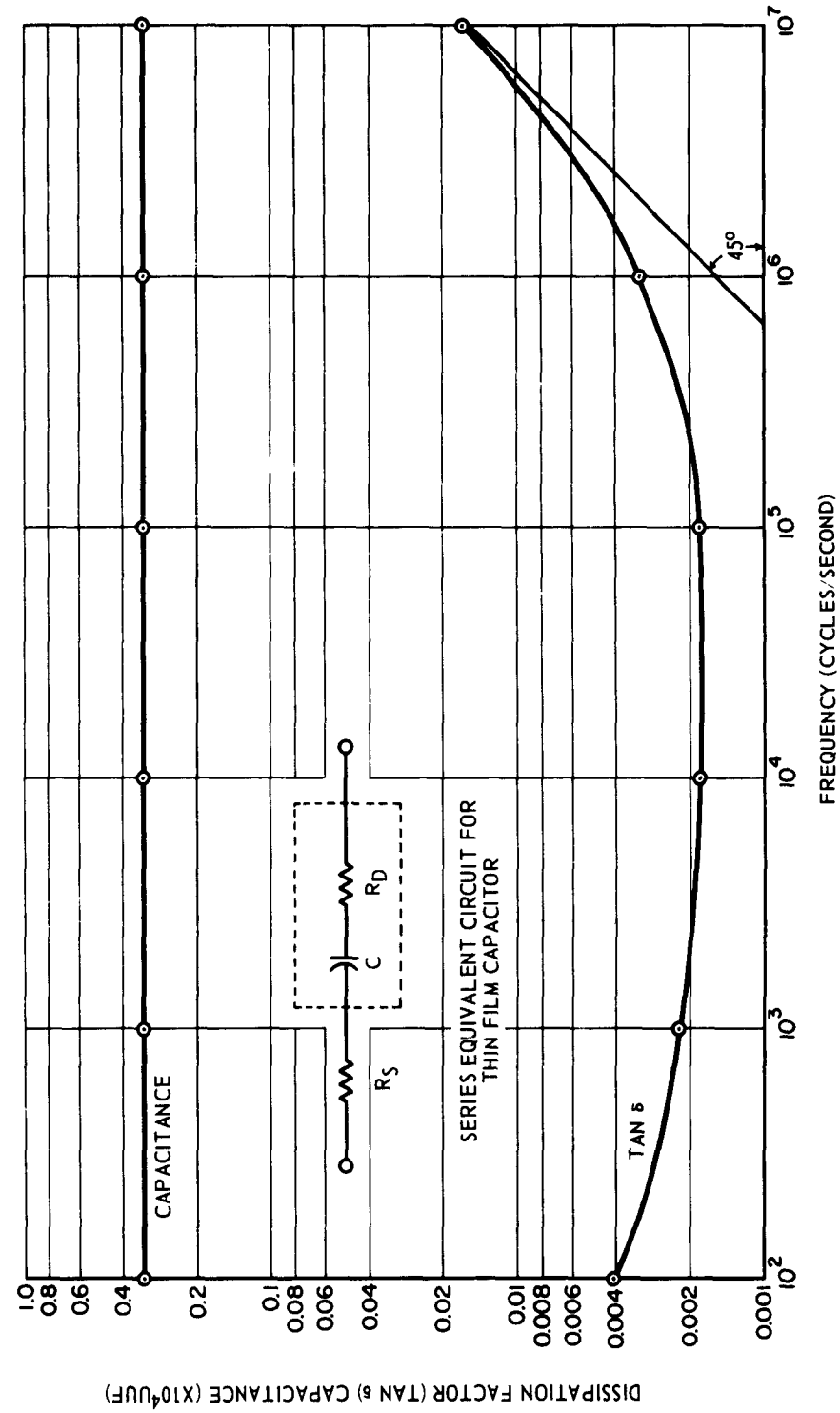

Figure 7. Frequency Dependence of an Nd_2O_3 Capacitor at Room Temperature

R5775

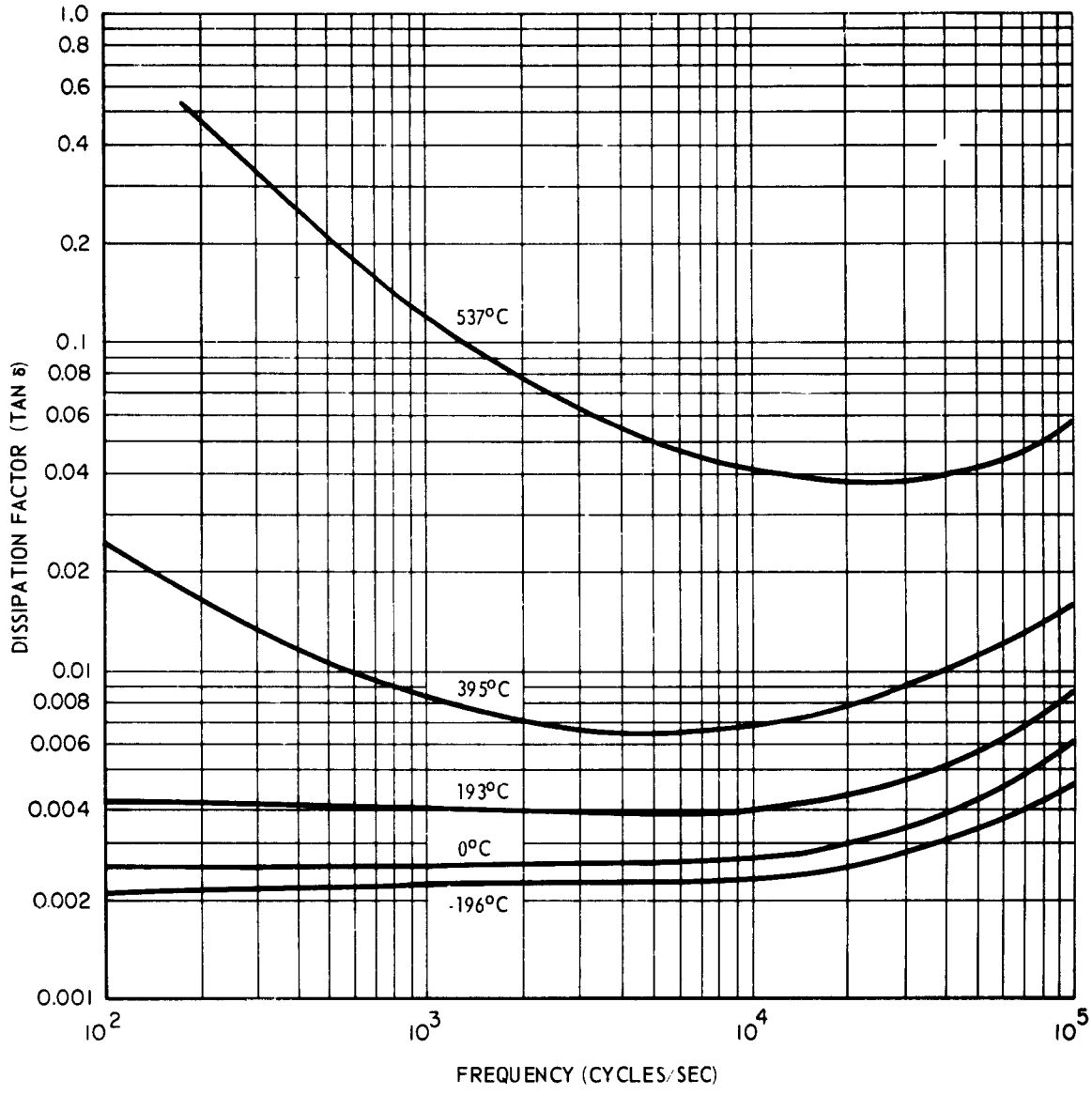

Figure 8. Frequency Characteristics of an Nd_2O_3 Capacitor at Various Temperatures

where R_D is the resistance of the dielectric itself and R_S represents all the rest of the series resistance between the terminals. Associated with these resistances, are the losses. Note that

$$\tan \delta_D = \omega C R_D \tag{2}$$

is the actual dielectric loss of the dielectric itself while $\omega C R_S$ represents the total of the lead, plate, and interconnection losses. These two contributions have definite physical significance and each has its own behavior.

It should be noted that the parallel equivalent circuit could be used in the analysis with similar results. However, such an analysis would be far more difficult to perform since the equations are considerably more cumbersome.

Considering first the dielectric loss, it becomes apparent, from figure 7 and other data, that tan δ is relatively independent of frequency in the low frequency region.[11] This is the region where the dissipation of the dielectric predominates,[12] and its insensitivity may indicate the presence of many elementary relaxation processes, each with their own characteristic relaxation times contributing to the losses. Thin-films of a glassy structure exhibit as the three basic causes of loss, inhomogeneity, dipole orientation, and ionic migration, all of which occasionally show variations in relaxation times, thus giving rise to a

---

11 M. Gevers and F. K. DuPre, Phillips Tech. Rev. 9 91 (1947)
12 D. A. McLean, J. Electochem. Soc. 108, 1, (1961)

frequency independent dissipation factor.[13] This can be verified experiementally by observing that, at low frequencies, one can change the series resistance R_S without appreciably affecting the dissipation factor $\tan\delta$, while at higher frequencies there is significant dependence of $\tan\delta$ on the series resistance.

On the other hand, it is the low frequency dissipation factor which is most sensitive to temperature change, as can be seen from figure 5. This is expected, since dielectric conductivity is much more temperature dependent than is metallic conductivity. Thus it is evident that at low frequencies the temperature behavior of $\tan\delta$ very closely approximates the temperature dependence of the actual dielectric loss, $\tan\delta_D$. It can be assumed that the series resistance is true ohmic resistance; thus the dissipation factor which would be observed if there were no dielectric loss is then ωCR_S. Since we are assuming a frequency independent dielectric loss, then we can assume that high frequency loss behavior is due solely to the series resistance. Frequency characteristics can be used to study comparative dielectric film quality at low frequencies, while plate and lead loss can be compared between capacitors at high frequencies.

To determine the true behavior of the dielectric loss as a function of frequency, an approximate method introduced by McLean[12] will be employed. Equations (1) and (2) can be combined, yielding

$$\tan\delta = \tan\delta_D = \omega CR_S \qquad (3)$$

---

13 J. B. Birks and J. H. Schulman, ed., Progress in Dielectrics, Vol II. John Wiley and Sons, Inc., New York (1960)

If the dissipation factor is validly expressed by equation (3), from the foregoing it is apparent that at low frequencies tan δ will behave principally as tan δ_D, i.e. frequency insensitive, while at higher frequencies ωCR_S will dictate the behavior of tan δ. This is clearly seen from figure 7, that tan δ approaches a 45° slope on the log tan δ versus log frequency curve. A 45° slope occurs only for an ideal situation where the capacitance is independent of the frequency. In practice, the capacitance does decrease slightly with increasing frequency, so we should expect the slope of tan δ to be slightly less than 45°. It should be noted here that if both tan δ_D and C are truly independent of the frequency, R_D must vary inversely as the frequency

$$R_D = \frac{A}{\omega C}$$

The values of tan δ_D and R_2 can be determined from the curve by substituting values of C and tan δ at two different frequencies.

$$\tan \delta_1 = \tan \delta_D + \omega_1 C_1 R_S$$

$$\tan \delta_2 = \tan \delta_D + \omega_2 C_2 R_S$$

and since tan δ_D is independent of the frequency, one can solve the two equations simultaneously. R_S, being frequency independent, can be calculated from

$$R_S = \frac{\tan \delta_1 - \tan \delta_2}{\omega_1 C_1 - \omega_2 C_2} \qquad (4)$$

Now the values for tan δ_D, the dielectric loss, can be found from

$$\tan \delta_D = \tan \delta - \omega C R_S = \tan \delta - \omega C \left[\frac{\tan \delta_1 - \tan \delta_2}{\omega_1 C_1 - \omega_2 C_2} \right] \qquad (5)$$

and plotted point for point.

There are certain factors which, according to McLean[12], should govern the choices of ω_1 and ω_2. The higher frequency, given in terms of ω_2, must not extend beyond the point at which the frequency dependence of the capacitance ceases to be linear. The low frequency choice should be in the region where tan δ_D predominates. Maddocks and Thun[14] chose frequencies in the region of the 45° slope. McLean suggests that, the wider the range of frequencies chosen, the greater the precision; however, he has found that good precision is attainable even for frequencies not far apart, so that one need not extend the frequencies until the slope approaches 45°.

2.4.7 Temperature Dependence of the Electrical Properties of Capacitors

Figure 9 presents the temperature characteristics of the dissipation factor and the dielectric constant from -196°C to 550°C. Above 500°C the capacitance increases very rapidly, while the increase in dissipation factor begins at about 425°C, although operation remains satisfactory to 500°C.

The two principal loss mechanisms of glassy substances are due to relaxation-loss at low frequencies and vibration-loss at high frequencies. Relaxation phenomena may be divided into three parts; conduction losses,

---

14 F.S. Maddocks and R.E. Thun, J. Electrochem. Soc., 109, 2, 1962

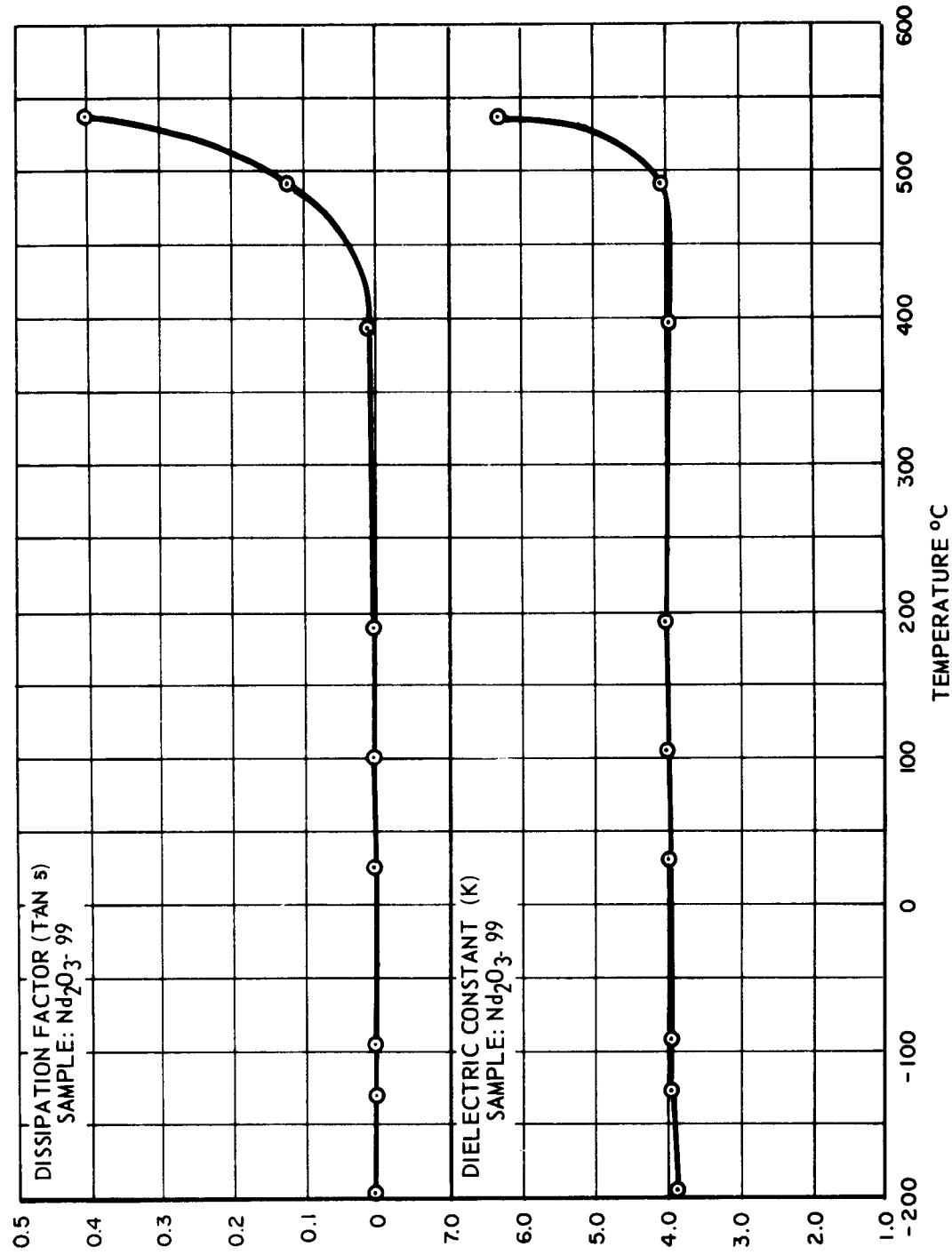

Figure 9. Dissipation Factor and Dielectric Constant vs. Temperature

dipole relaxation losses, and deformation losses, all of which depend on ion displacement and the kind of ion motion taking place. The losses due to conduction involve ionic migration over relatively large distances, in which some energy is given up to the lattice. The resistivity, δ, of glassy structures decreases rapidly with temperature and its dependence on temperature can be expressed as

$$\log \delta = A + \frac{6}{T} \tag{6}$$

Ion motion over short distances causes dipole relaxation losses. These losses predominate over the conduction losses beyond 100 cps and can be important up to 10^6 cps. This loss is generally of the form

$$\tan \delta_D = A \exp (BT) \tag{7}$$

Deformation losses involve even more limited motions, usually of whole networks of atoms, and predominate at high frequencies.

The dielectric resistance decreases as temperature rises, due to the increase in conduction loss, as seen in equation (6). From equation (7), the exponential dependence of the loss on temperature is evident. From equation

$$C = \frac{\tan \delta}{\omega(R_S+R_D)}$$

and since R_D decreases and tan δ_D increases, the temperature dependence of the capacitance is predicted. In figure 8 one observes a more temperature-dependent loss at low frequencies than at high frequencies. This is indicative of losses due principally to local movements of ions, corresponding to dipole relaxation mechanism.[5]

The temperature characteristics of the DC dielectric breakdown strength are illustrated in figure 10. The breakdown strength was found to be constant with temperature up to 560°C, a result which indicates that the resistivity is still very high at these elevated temperatures. The theory of breakdown due to localized dielectric heating is not supported in this case, since there is no apparent dependence of the breakdown strength on temperature for these films.[5] The resistivities of these films were measured at 550°C to be 1.4×10^{11} ohm-cm.

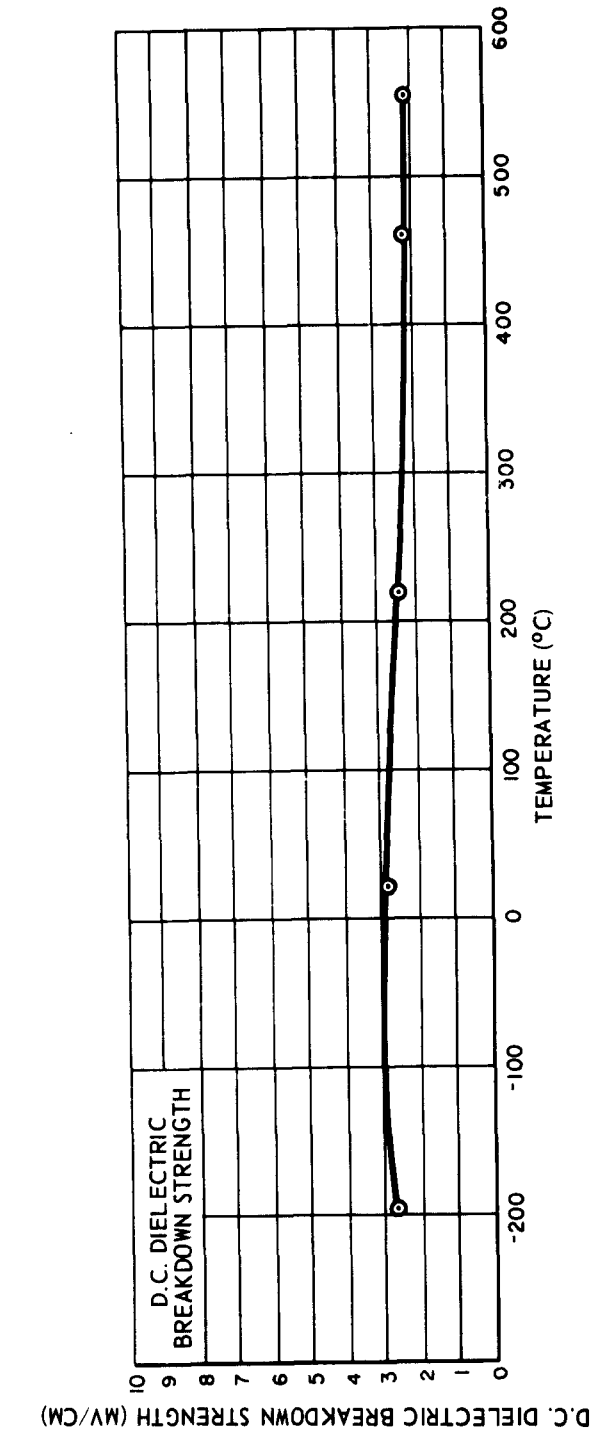

Figure 10. Dielectric Breakdown Strength vs. Temperature

2.5 Boron Films

Studies were resumed this quarter on vacumn deposited boron fims. Previous work on boron films was reported in the Third Quarterly Report, February 15, 1961. At that time efforts were being made to form crystalline films through variations in deposition techniques. However, results did not appear very encouraging and research on boron was postponed in favor of other materials. A new approach which has a great deal of promise has been taken this quarter. Instead of attempting to form crystalline fims and treating the material as a normal semiconductor, amorphous films have been formed and studied. The impetus for the study of amorphous boron films stems from the hope of forming longitudinal field effect devices in which the electrons pass through the boron layers. The low atomic number, low density, high melting point, and stability make boron a worthwhile material to study.

2.5.1 Deposition Techniques

Boron was deposited in vacumn by means of a focused electron beam. Various sources of boron were used and the deposition techniques varied somewhat, depending on the shape of the sample. Zone-refined boron having quoted purities of 99.9999% was used through the study. Some samples of boron were in the shape of rods, while others were in small crystalline lumps obtained quite a few years ago from the Eagle-Picher Co. The zone-refined rods were obtained both from A. D. Mac Kay, Inc. and Eagle-Picher. Five or six types of boron were tested but only one appeared to give good results. A few of the boron samples flew apart when bombarded with a beam, while others melted quite uniformly. Despite the purities quoted, spectroanalytical tests of the boron revealed quite a few impurities. Of all the materials tested, only the most pure gave desirable results. Analyses of four of the materials tested are given in table II.

TABLE II

Spectrographic Analyses of Boron Source Material

	No. 1	No. 2	No. 3	No. 4
Aluminum	W	T	X	X
Boron	Major	Major	Major	Major
Calcium	T	T	T	T
Copper	W	T	T	T
Germanium	W	T (low)	T (low)	X
Iron	T	T	T	X
Magnesium	T (low)	W	T	T (low)
Silicon	W	T	T	T (low)
Zinc	T	T	T	T

CODE:

X Not Detected < 0.001%
T Trace < 0.01%
W Weak 0.01-0.5%

Sample No. 1 Boron float-zoned, Eagle-Picher, 99.9999%, remelted in boron nitride liner.

Sample No. 2 Boron float-zoned bar, Eagle-Picher, 99.9999% not melted.

Sample No. 3 Boron, Eagle-Picher, Sample M5910AV

Sample No. 4 Boron, Eagle-Picher, Sample M5910AW

From past experience, it was known that deposition of boron at low substrate temperatures yielded amorphous layers. The situation is similar to that found for both silicon and germanium reported extensively in previous reports. Below certain substrate temperatures, silicon and germanium as well as boron remains quite high until these critical temperatures are reached. In the cases of boron and silicon, the temperatures are quite high (over 1000°C) and consequently crystalline films are difficult to form. In contrast, germanium films begin to crystallize at approximately 350°C. The boron fims used in this study were deposited on substrates of fused silica or glass held at room temperatures.

In order to study the electron transmission through the boron layers, the boron was deposited between evaporated metal layers on the substrate. Sixteen samples were deposited at one time on one inch square substrates. Generally, aluminum electrodes were employed. Each sample thus forms a small condensor a few square millimeters in area. In this initial study and in an effort to keep the boron deposition chamber as clean as possible, the metal electrodes were deposited in a separate chamber. This means that the sample was exposed to air twice before it was completed.

2.5.2 Electrical Properties

Boron samples of the best purity material (No. 4 in table II) were deposited in thicknesses from five hundred to several thousand angstroms. The electrical resistivity of even the thinnest sample was quite high ($\sim 10^{11}$ Ω-cm). The characteristics of the sample were first displayed on a Tektronics Type 575 curve tracer. Typical characteristics are shown in figure 11. Note the relatively flat region showing low conductivity until a critical voltage was applied across the sample. Over-voltages as much as 10 to 100 times that near the critical

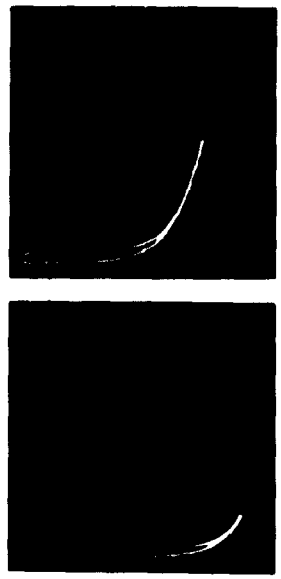

FILM THICKNESS 1100Å BORON 3 LAYER DEVICE

TOP CHARACTERISTIC SAMPLE AT ROOM TEMP.
BOTTOM CHARACTERISTIC SAMPLE AT LIQUID N_2 TEMP. (77°K)
VERTICAL SCALE .02MA/DIV
HORIZONTAL SCALE 2V/DIV

Figure 11. I-V Characteristics of a Boron Three-Layer Device

voltage could be applied without breaking down the sample. The characteristics at liquid nitrogen temperature are also shown in figure 11. As might be expected, the threshold or steep portion of the curve shifted to higher field values. Typical current-voltage characteristics at various temperatures are shown in figure 12. The data for this figure were obtained by point measurements.

Because of the very nonlinear characteristics of the boron films, one of the samples was evaluated as a voltage limiting device in the circuit shown in figure 13. In this circuit, the top electrode has a resistance of some nominal value. As the voltage through this resistor increases, a point is reached where the current suddenly begins to be drawn by the plate through the boron film. This serves the function of clipping the sine wave at a particular voltage which is determined by the thickness of the boron layer. The accompanying oscilloscope trace in figure 13 illustrates the effectiveness of this approach. Three-layer devices of this sort will certainly be applicable to circuits which require simple voltage limiting devices.

2.5.3. Discussion

Because of the interesting nonlinear characteristics of these amorphous boron films and because other semiconducting films when deposited at low temperatures are amorphous, similar samples were made using germanium, silicon, boron, and silicon carbide amorphous films. The silicon carbide was formed by sputtering, while the other films were formed by vacuum deposition. The results of these tests are shown in figure 14, which is a log-log plot in order to accomodate all the data. Of these materials, boron was the only one that showed a very sharp break above a certain critical voltage. (This is difficult to see in the figure). It is interesting to note that the higher the band gap of the bulk material, the more field is required to obtain the same current.

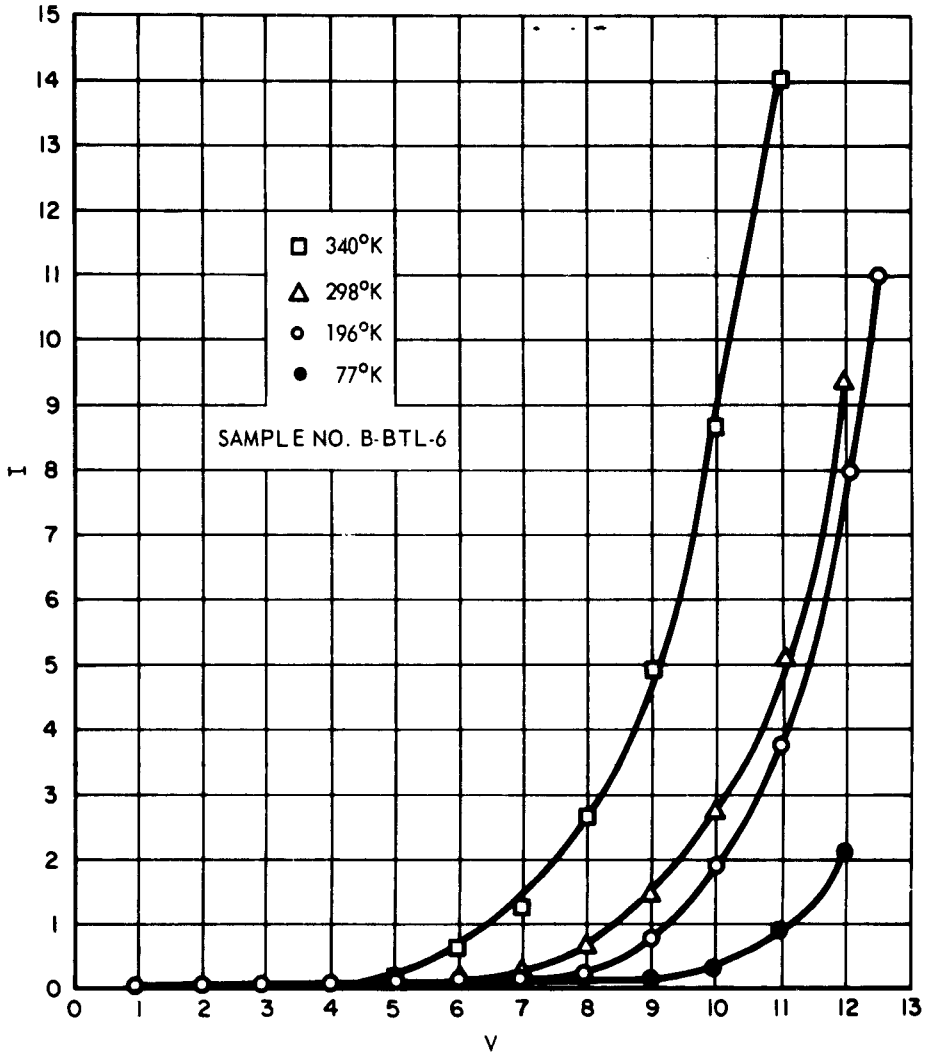

Figure 12. I-V Characteristics of a Boron Three-Layer Device at Several Temperatures

FILM THICKNESS 1800Å BORON 3 LAYER DEVICE

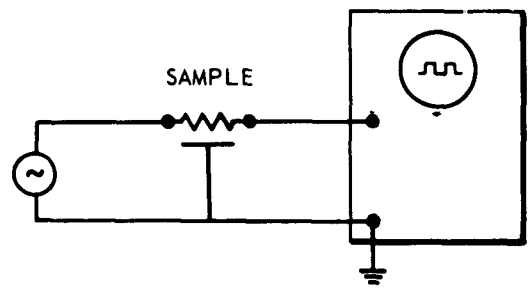

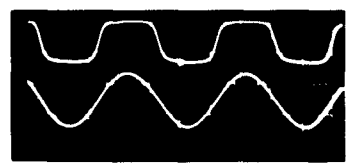

VERTICAL SCALES
TOP TRACE 20V/CM.
BOTTOM TRACE 50V/CM

Figure 13. Schematic Diagram and Input and Output Wave Forms of Clipping Circuit Using a Boron Three-Layer Device

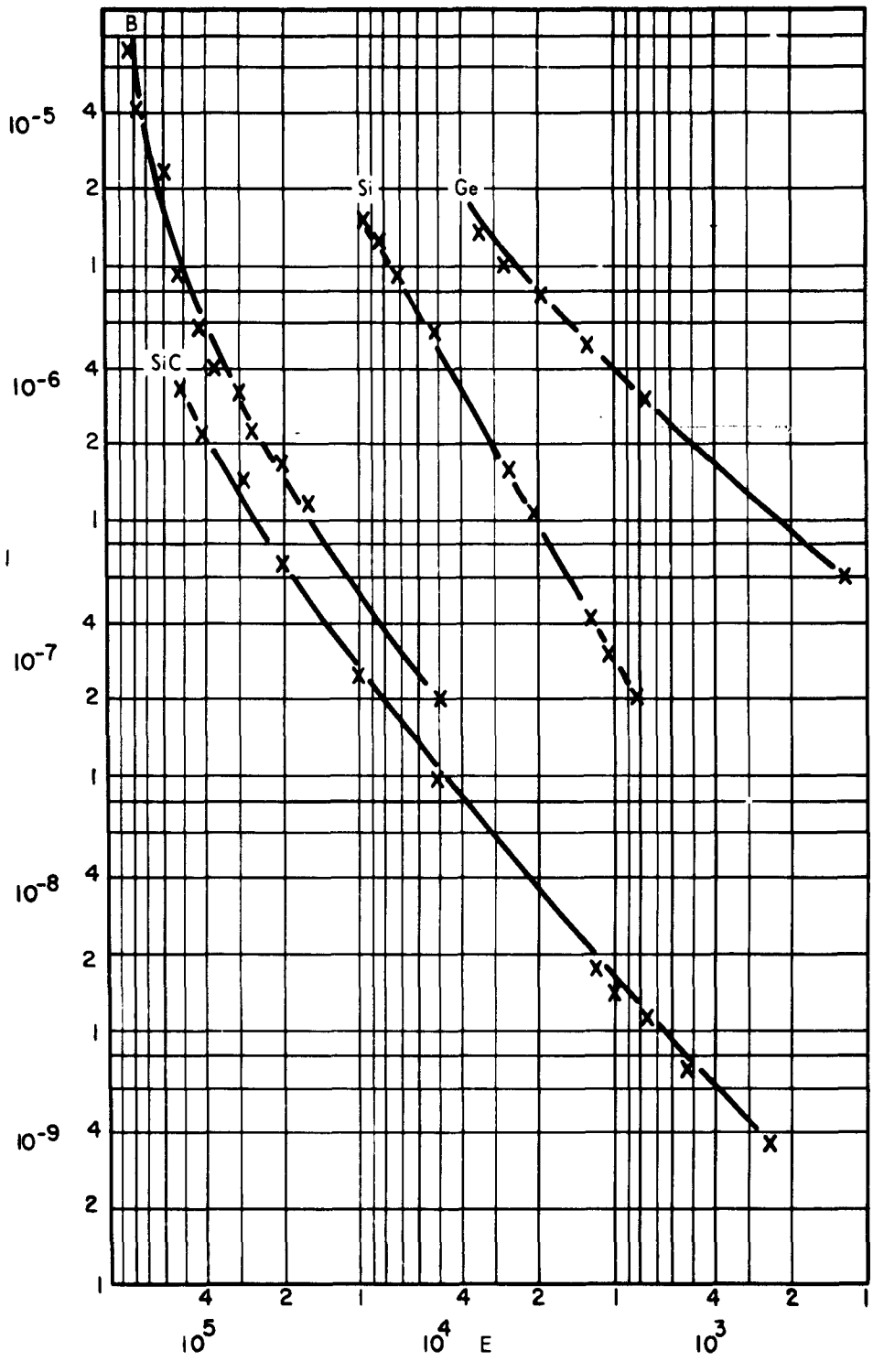

Figure 14. I-E Characteristics of Several Amorphous Materials

Unfortunately, the boron material which gave the best results has been expended, but attempts to find other suitable materials are underway. Because of the limited number of samples tested and the limited results obtained, the interpretation of this data will be left to subsequent reports. The thickness of the films rules out a tunneling phenomenon. Other phenomenon, such as field emission, internal field emission, avalanche breakdown, or simply variations of mobility with field in amorphous materials, may be present. It is hoped that a careful analysis of the data with subsequent samples will aid in understanding the phenomena.

3. MICRODEVICE RESEARCH

Improvements continue to be realized in the formation of thin film field effect devices. In particular, reliable devices using thinner semiconductor layers have been produced with a greater consistency than had heretofore been the case. It is now recognized that the type of dielectric film used has a profound effect on the properties of the finished device; reasons for this behavior are presently being explored.

Two papers on field effect devices were presented at the recent meeting ot the Electrochemical Society, held in Pittsburgh, Pa., on the 15th through 18th of April. These were as follows:

"A Germanium Thin Film Field Device, "by H. L. Wilson, W. T. Layton, W. A. Gutierrez and C. Feldman (delivered by W. T. Layton)

"Cadmium Selenide Thin Film Field Effect Transistors, " by H. L. Wilson and W. A. Gutierrez (delivered by H. L. Wilson).

3.1 Thin Film Device Characteristics

Further improvements in the electrical characteristics of field effect devices were accomplished during this quarter, particularly for those incorporating a CdSe semiconductor layer. Figure 15 exhibits the characteristic curves of a CdSe device formed early in this quarter. The input resistance of this device was approximately 200 megohms. SiO_2 was utilized as the dielectric film in the device. Later in the quarter even greater transconductances were achieved - up to 500 μmhos for the same configuration; however, such devices showed hysteresis in the stepped I_d versus V_d characteristics. The semiconductor layers of such devices ranged from 300 to 1500 Å in thickness.

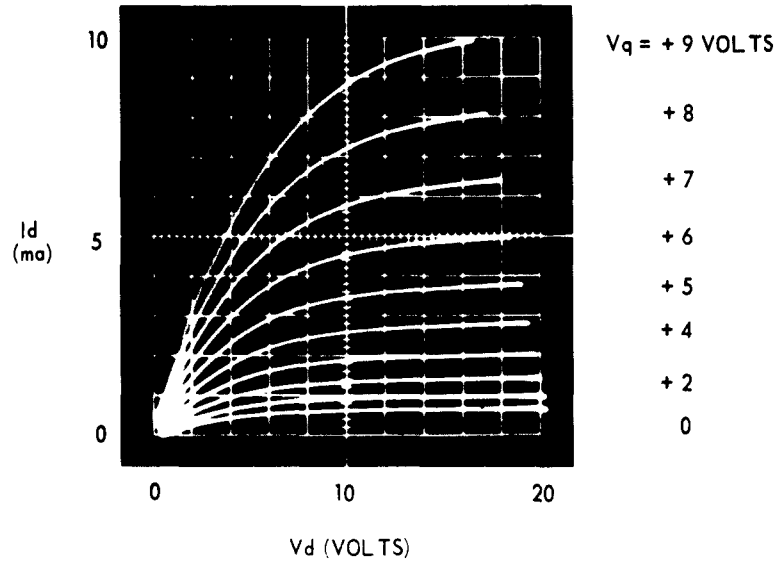

Rd ~ 100K Ω
Gm ~ 1000 μmhos
μ ~ 100
Cin ~ 100 pf
Rin ~ 100 Meg Ω
GB ~ 2MC

Figure 15. I_D-V_D Characteristics of a CdSe Device Operating in the Enhancement Mode

All device characteristics shown, in this and previous quarterly reports, refer to devices with source-drain spacings of 0.5 mil and source-drain interfaces (device width) of 100 mils. This is to be noted, since values of transconductance, input and output impedance, and capacitance are dependent on both the geometry and dimensions of the sample.

No significant improvements in CdS or CdTe devices were realized this quarter over those previously reported. The suppliers from whom high purity CdTe is available are few in number and cost of this material is approximately 10 times that of CdS or CdSe.

In quarterly report No. 11 (pages 15-17) the resistance behavior of a CdSe film during device formation was described. Of particular interest was the sudden drop of CdSe film resistance when the overlying dielectric was applied. This sharp decrease in resistance also occurs with both CdS and CdTe films. Drops in resistance in CdS and CdSe films of up to 10,000 to 1 have recently been observed.

It has been noted this quarter that this resistance drop varies with the application of different dielectrics (i.e. SiO, SiO_2, La_2O_3), which may imply that certain dielectrics are preferable for use with these devices. This could, of course, be due to differing deposition parameters or surface characteristics. It is also possible that differing stresses in the overlying dielectric layer used create different secondary stresses in the semiconductor film structure, thereby changing its electrical and physical properties. Determination of the exact reason for the sudden drop in semiconductor resistance might, in any case, provide a clue for substantiating the operating mechanism for the device.

3.2 Thermal Properties of Thin-Film Devices

Cadmium selenide devices have been examined again this quarter to determine thermal stability. The experimental arrangement is the same as that reported in the eleventh quarterly. One of the devices tested had SiO_2 dielectric layer, which should allow device operation to higher temperatures than SiO. The source-drain resistance of the sample was high (about 1 megohm) and necessitated a large drain voltage. This, together with the comparatively small, positive gate potential, resulted in a large potential drop between the gate and the drain side of the semiconductor. This large electric field led to device breakdown at the low temperature of 84°C.

Another CdSe device tested had a neodymium oxide dielectric layer. Relatively large potentials had to be applied in order to obtain observable I_d-V_d curves. These led, in turn, to large dissipation current densities, which caused device breakdown at a low temperature (130°C).

In the Eleventh Quarterly Report (Section 3.1.1, page 33) it was stated that "The slopes of the curves obtained with a cadmium sulfide and a cadmium slenide device yielded calculated thermal band gaps of 2.9 ev and 1.4 ev, respectively." This statement was made in relation to the sulfide and selenide devices whose thermal stability was determined. On recalculating the thermal band gaps, it was found that an arithmetic error had been made. The correct balues are, respectively, 1.04 ev and 1.48 ev.

4. FUNCTION SYNTHESIS STUDIES

This section has been initiated to give an increased emphasis to the phases of work previously discussed as Field Effect Circuit Characteristics. During this quarter, a thin-film field effect device was tested in a current limiter circuit. Comparisons are made between certain predictions of equations derived on the basis of a theoretical model of the device and operating characteristics of the circuit.

4.1 A Current Limiter Application of the Thin-Film Triode

With the advent of thin-film circuitry, thin-film active and passive elements exhibiting useful circuit functions have been of great interest. An analysis of the insulated-gate thin-film triode used as a current limiter is described in this section.

The application of the field effect device as a current limiter was proposed as early as 1958 by R.M. Warner, Jr.[15] The device is in essence a self-biased field effect transistor operating in the depletion mode.

Consider an insulated-gate thin-film triode connected as shown in figure 16. Since the current is from drain to source, the semiconductor channel acquires a positive potential with respect to the grounded field plate. This potential varies from a maximum of V at the drain to zero at the source. The effect of this potential gradient in the X direction is to reverse-bias the channel, assuming an N-type semiconductor channel, and to set up a depletion layer of thickness h, which varies as a function of the potential distribution in X. Thus, the effective thickness of the conducting channel is reduced as the applied voltage is increased. When the depletion layer extends across the total thickness of the semiconductor,

---

15 R.M. Warner, Jr., 1958 IRE National Convention Record, 6, pt. 3, pp. 43-48 (1958)

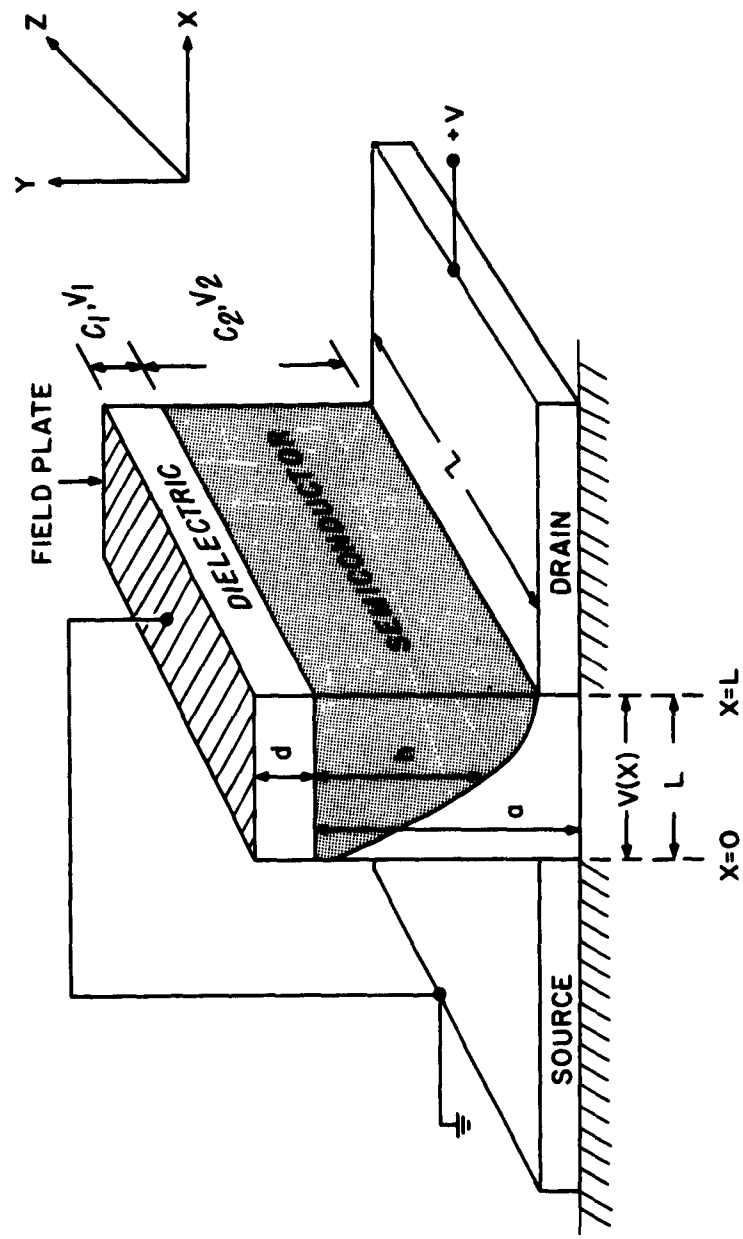

Figure 16. Depletion Layer in Self-Biased Field Effect Unit

"pinch-off" is achieved. The voltage at which this occurs is called the pinch-off voltage, V_p. Further increases in applied potential have very little effect on the effective thickness of the channel and the current becomes constant. This constant current condition will persist until the applied voltage is large enough to cause breakdown. Figure 17 illustrates qualitatively the I-V characteristics of the current limiter.

An application of the current limiter makes use of its constant current characteristics. Placed between a power supply and its load, it will maintain constant current, despite variations in supply voltage or load impedance. Transient disturbances will also be suppressed. Due to its high ratio of ac-to-dc resistance, the device can also be used for discrimination between ac and dc, the operating frequency being limited by the combination of dielectric and depletion layer capacitances, as well as by the recombination, lifetime and mobility of the current carriers. The current limiter may also be used for circuit overload protection and for certain wave shaping functions.

Model of the Insulated-Gate Thin Film Triode Current Limiter: A theoretical treatment of the essential features of the insulated-gate, thin-film triode current limiter will be considered in this section. The geometrical model to be discussed is that shown in figure 16. An essential consideration in this treatment is that the field plate is separated from the semiconductor channel by a dielectric of thickness d. It is necessary to calculate the potential across the depletion layer in the y direction as a function of the channel potential in the X direction.

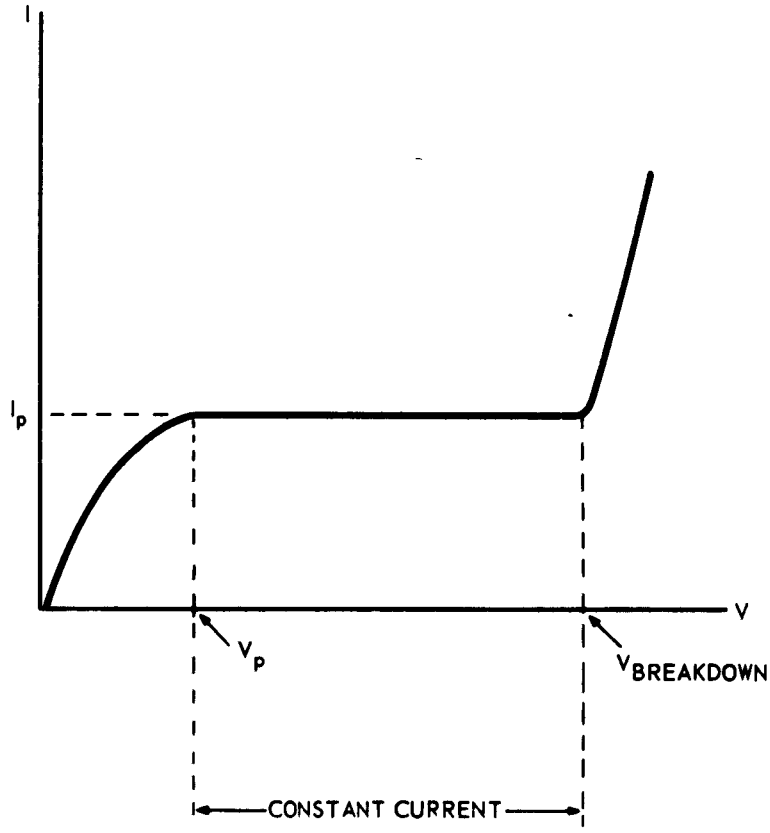

Figure 17. I-V Characteristic of the Current Limiter

With the source grounded and current flowing from drain to source, a depletion layer of thickness h is developed in the semiconductor, due to the reverse bias condition that exists between field plate and semiconductor. The thickness of the depletion layer h is a function of X. More specifically, h is a function of the voltage v_2 developed across the depletion layer in the y direction. This, in turn, is a function of the potential v(x) at any point X in the semiconductor. Assuming a uniform and completely ionized impurity density in the semiconductor, the potential across the depletion layer may be calculated from Poisson's equation and the solution written as

$$v_2 = \frac{qNh^2}{2k_2\varepsilon_o} \tag{1}$$

where N is the impurity density, h is the depletion layer thickness, k_2 is the dielectric constant of the semiconductor material, and ε_o is the permittivity of free space.

It now becomes necessary to calculate the relation between v_2 and the potential in the channel v(x) in order to obtain a relationship between v(x) and h. Considering figure 16, the potential in the channel v(x) is the applied potential and is given by

$$v(x) = v_1 + v_2 \tag{2}$$

where v_1 is the potential across the dielectric. Considering C_1, the capacitance of the dielectric to be in series with C_2, the capacitance of the depletion layer, v_2 may be written as

$$v_2 = \frac{C_1}{C_1 + C_2} \quad v(x) \tag{3}$$

where

$$C_1 = \frac{k_1 \varepsilon_o Zh}{d} \tag{4}$$

and

$$C_2 = \frac{k_2 \varepsilon_o Zh}{h} \tag{5}$$

k_1 being the dielectric constant of the dielectric material, h being the length of the channel and Z its width, d the dielectric thickness, and h the depletion layer thickness. Substituting equations (4) and (5) into (3) results in

$$v_2 = \frac{k_1 \, h}{k_1 \, h + k_2 d} \quad v(x) \tag{6}$$

Inserting relationship (6) into (1) results in

$$v(x) = \frac{qN}{2k_2 k_1 \varepsilon_o} \left[k_1 h^2 + k_2 \, dh \right] \tag{7}$$

and letting

$$\beta = \frac{2k_2 k_1 \varepsilon_o}{qN} \tag{8}$$

one can then write equation (7) as

$$h^2 + \left[\frac{k_2 d}{k_1} \right] h + \left(- \frac{\beta}{k_1} \right) v(x) = 0 \tag{9}$$

For simplicity, let

$$b = \frac{k_2 d}{k_1} \tag{10}$$

and

$$c = -\frac{\beta}{k_1} \tag{11}$$

Solving equation (9) for h, one obtains

$$h = \frac{-b + (b^2 + 4\, cv(x))^{1/2}}{2} \tag{12}$$

Since negative values of h are physically impossible, only the positive value of the square root is considered. Equation (12) describes how the depletion layer thickness h varies with the channel potential v(x). As the potential applied to the drain is increased, the depletion layer thickness increases until it extends completely across the channel. The voltage at which this occurs is called the pinch-off voltage and is given by

$$v_p = \frac{a(a + b)}{c} \tag{13}$$

where a is the thickness of the channel and b and c are defined by (10) and (11) respectively.

The current density in the channel is given by Ohm's law.

$$\vec{J}(x) = \delta \vec{E}(x) = \delta \frac{dv}{dx} \tag{14}$$

where δ is the conductivity of the channel. The current density may be expressed in terms of the depletion layer thickness as

$$\vec{J}(x) = \frac{\vec{I}}{Z(a-h)} \tag{15}$$

where Z is the width of the channel. Inserting (15) into (14) one obtains

$$\frac{dv}{dx} = \frac{\vec{I}}{\delta Z(a-h)} \tag{16}$$

Inserting (12) and (13) into (16) leads to

$$\left[(b^2 + 4cV_p)^{1/2} - \left((b^2 + 4cv(x)\right)^{1/2}\right] \frac{dv}{dx} = \frac{2\vec{I}}{\delta Z} \tag{17}$$

Equation (17) may be integrated and rearranged to yield

$$6cv(x)\,(b^2 + 4cV_p)^{1/2} - \left((b^2 + 4cv(x)\right)^{3/2} = \frac{12\,clx}{\delta Z} - b^3 \tag{18}$$

This defines the potential in the channel in terms of measureable parameters. The boundary condition, $v(x) = 0$ at $x = 0$ has been used to obtain the constant of integration. From (18) the current in the channel as a function of the voltage V applied to the drain is given by

$$I = \frac{\delta Z(2a + b)}{12\,CL}\left\{6cV + \frac{b^3}{(2a+b)} - \left(\frac{b^2 + 4cV}{b^2 + 4cV_p}\right)^{1/2}(b^2 + 4cV)\right\} \tag{19}$$

At the pinch-off voltage V_p, equation (19) reduces to

$$I_p = \frac{\delta Z(2a + b)}{12\, cL} \left(2cV_p + \frac{b^3}{(2a + b)} - b^2 \right) \qquad (20)$$

where I_p is the pinch-off current.

Hence (13) and (20), respectively, give the minimum value of the voltage necessary for pinch-off and current value at pinch-off. Equation (19) gives the I-V characteristics of the insulated gate current limiter in terms of measureable parameters.

The small signal ac resistance $\frac{dV}{dI}$ may be obtained by differentiating equation (19). The dc resistance $\frac{V}{I}$ may be obtained by dividing (19) into the applied drain voltage.

Comparison with Experiment: The equations derived in the previous section have been applied to a CdS_e thin-film triode used as a current limiter. The primary objective was to compare calculated values of V_p and I_p with values determined experimentally. From this, conclusions can be drawn regarding the validity of the equations and assumptions made in their derivation.

A thin film CdSe current limiter had the following parameters:

$a = 1000$ Å

$d = 1000$ Å

$k_1 \simeq 5$

$k_2 \simeq 10$

$h = 10 \times 10^{-4}$ cm

$Z = 0.254$ cm

$\rho = 254$ ohm-cm

$\mu_D = 1$ cm^2/v-sec.

Bulk values have been used for k_1 and k_2; film values may differ considerably. The value for μ_D is assumed for the sample, but considered reasonable in light of Hall measurements on CdSe films. Calculated values of V_p and I_p for this unit were 0.79 volts and 3μa, respectively. This may be compared with the experimental values for V_p and I_p of approximately 1 volt and 6μa, respectively. The comparisons are reasonable considering the approximations made for dielectric constant and mobility. In order to fully substantiate the validity of the theoretical treatment, more current limiting devices will have to be prepared and evaluated.

It should be noted that no particular effort was made to fabricate a useful thin-film current limiter. Regulation at 6μa is not large enough to be useful, even though the pinch-off voltage is quite low. However, by controlling the resistivity of the semiconductor, by depositing different thicknesses of semiconductor and dielectric, and possibly by applying a positive bias potential between field plate and ground, useful current limiters that would regulate at higher currents with reasonable pinch-off voltages could perhaps be fabricated. Effects due to photosensitivity, drift, power dissipation, aging, and environment on the performance of the current limiter must also be considered.

5. CONCLUSIONS

There has been a gradual shift of emphasis during the course of this program from materials research through effects and devices, to functional syntheses. A new section was started for this quarterly report in order to "break out" the functional syntheses or circuit analyses from the purely physical research aspects of the contract. Some work has, of course, been reported in previous reports on circuit functions, but was included in microdevice sections. This should aid in the usefulness of these quarterly reports. This month, the field effects have been explored as a current limiting device. In the ensuring months, similar projects will be carried out. The work on field effect devices, of course, will be pursued, since a good deal of information is lacking on both the fabrication and physics involved. New materials, such as boron, and effects in materials are constantly being considered and explored in order to meet the desired goals. Those materials which do not appear promising are usually postponed or dropped. Work on sputtering and vapor deposited films continues at a low level of effort in order to provide additional information on both materials and effects. Work on dielectrics has finally yielded a material that appears to be suitable for forming insulting films to operate up to 500°C. Studies of neodymium oxide are quite incomplete and will be continued throughout the next quarter. If the materials still appear to meet the ultimate goals, a complete electrical characterization of the material will be carried out. A small effort is being continued on the fabrication of test samples and circuits for radiation testing. The results of these tests, as in the past, are being reported elsewhere.

Senior personnel now participating in work on this contract are:

Mr. Stanley M. Bryla

Dr. Charles Feldman

Mr. Charles Gane

Mr. Michael Hacskylo

Mr. Wilbur T. Layton

Dr. Maurice M. Mitchell, Jr.

Dr. Charles W. Moulton

Mr. Herbert L. Wilson

Prepared by: Charles W. Moulton

Charles W. Moulton
Principal Chemist

Approved by: Charles Feldman

Charles Feldman
Head, Physical Electronics Section

Howard S. Coleman

Howard S. Coleman
Head, Physics Research

P. E. Ritt

P. E. Ritt
Vice President - Research